New Journal of Physics
The open access journal at the forefront of physics

Deutsche Physikalische Gesellschaft DPG
IOP Institute of Physics

Published in partnership with: Deutsche Physikalische Gesellschaft and the Institute of Physics

OPEN ACCESS

RECEIVED
1 December 2015

REVISED
16 February 2016

ACCEPTED FOR PUBLICATION
22 February 2016

PUBLISHED
24 March 2016

PAPER

Electroweak breaking and neutrino mass: 'invisible' Higgs decays at the LHC (type II seesaw)

Cesar Bonilla[1,3], **Jorge C Romão**[2] **and José W F Valle**[1]

[1] AHEP Group, Instituto de Física Corpuscular — C.S.I.C./Universitat de València Edificio de Institutos de Paterna, C/Catedratico José Beltrán, 2 E-46980 Paterna (València) - Spain
[2] Departamento de Física and CFTP, Instituto Superior Técnico Universidade de Lisboa, Av. Rovisco Pais 1, 1049-001 Lisboa, Portugal
[3] Author to whom any correspondence should be addressed.

E-mail: cesar.bonilla@ific.uv.es, jorge.romao@tecnico.ulisboa.pt **and** valle@ific.uv.es

Keywords: neutrino mass, invisible Higgs decays, Higgs physics

Abstract

Neutrino mass generation through the Higgs mechanism not only suggests the need to reconsider the physics of electroweak symmetry breaking from a new perspective, but also provides a new theoretically consistent and experimentally viable paradigm. We illustrate this by describing the main features of the electroweak symmetry breaking sector of the simplest type-II seesaw model with spontaneous breaking of lepton number. After reviewing the relevant 'theoretical' and astrophysical restrictions on the Higgs sector, we perform an analysis of the sensitivities of Higgs Boson searches at the ongoing ATLAS and CMS experiments at the LHC, including not only the new contributions to the decay channels present in the standard model (SM) but also genuinely non-SM Higgs Boson decays, such as 'invisible' Higgs Boson decays to majorons. We find sensitivities that are likely to be reached at the upcoming run of the experiments.

1. Introduction

The electroweak breaking sector is a fundamental ingredient of the standard model (SM), many of whose detailed properties remain open even after the historic discovery of the Higgs Boson [1, 2]. The electroweak breaking sector is subject to many restrictions following from direct experimental searches at colliders [3, 4], as well as global fits [5, 6] of precision observables [7–9]. Moreover, its properties are may also be restricted by theoretical consistency arguments, such as naturalness, perturbativity and stability [10]. The latter have long provided strong motivation for extensions of the SM such as those based on the idea of supersymmetry.

Following the approach recently suggested in [11, 12] we propose to take seriously the hints from the neutrino mass generation scenario to the structure of the scalar sector. In particular, the most accepted scenario of neutrino mass generation associates the small size of the neutrino mass to their charge neutrality which suggests them to be of Majorana nature due to some, currently unknown, mechanism of lepton number violation. The latter requires an extension of the $SU(3)_c \otimes SU(2)_L \otimes U(1)_Y$ Higgs sector and hence the need to reconsider the physics of symmetry breaking from a new perspective. In broad terms this would provide an alternative to supersymmetry as a paradigm of electroweak breaking. Amongst its other characteristic features is the presence of doubly charged scalar bosons, compressed mass spectra of heavy scalars dictated by stability and perturbativity and the presence of 'invisible' decays of Higgs Bosons to the Nambu-Goldstone boson associated to spontaneous lepton number violation and neutrino mass generation [13].

In this paper we study the invisible decays of the Higgs Bosons in the context of a type-II seesaw majoron model [14] in which the neutrino mass is generated after spontaneous violation of lepton number at some low energy scale, $\Lambda_{EW} \lesssim \Lambda \sim \mathcal{O}(\text{TeV})$ [15, 16][4]. This scheme requires the presence of two lepton number carrying scalar

[4] The idea of the Majoron was first proposed in [17] though in the framework of the type I seesaw, not relevant for our current paper. On the other hand the triplet Majoron was suggested in [18] but has been ruled out since the first measurements of the invisible Z width by the LEP experiments. Regarding the idea of invisible Higgs decays was first given in [19], though the early scenarios have been ruled out.

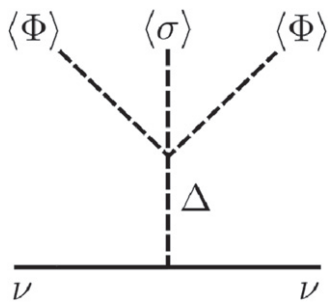

Figure 1. Diagram that generates non-zero neutrino mass in the model.

multiplets in the extended $SU(3)_c \otimes SU(2)_L \otimes U(1)_Y$ model, a singlet σ and a triplet Δ under SU(2)—this seesaw scheme was called '123'-seesaw model in [14] and here we take the 'pure' version of this scheme, without right-handed neutrinos. The presence of the new scalars implies the existence of new contributions to 'visible' SM Higgs decays, such as the $h \to \gamma\gamma$ decay channel, in addition to intrinsically new Higgs decay channels involving the emission of majorons, such as the 'invisible' decays of the CP-even scalar bosons. As a result, one can set upper limits on the invisible decay channel based on the available data which restrict the 'visible' channels.

The plan of this paper is as follows. In the next section we describe the main features of the symmetry breaking sector of the '123' type II seesaw model. In section 3 we discuss the 'theoretical' and astrophysical constraints relevant for the Higgs sector. Taking these into account, we study the sensitivities of Higgs Boson searches at the LHC to Standard Modelscalar boson decays in section 4. Section 5 addresses the non-SM Higgs decays of the model. Section 6 summarizes our results and we conclude in section 7.

2. The type-II seesaw model

Our basic framework is the '123' seesaw scheme originally proposed in [14] whose Higgs sector contains, in addition to the $SU(3)_c \otimes SU(2)_L \otimes U(1)_Y$ scalar doublet Φ, two lepton-number-carrying scalars: a complex singlet σ and a triplet Δ. All these fields develop non-zero vacuum expectation values (vevs) leading to the breaking of the Standard Model(SM) gauge group as well as the global symmetry $U(1)_L$ associated to lepton number. The latter breaking accounts for generation of the small neutrino masses.

Therefore, the scalar sector is given by

$$\Phi = \begin{bmatrix} \phi^0 \\ \phi^- \end{bmatrix} \quad \text{and} \quad \Delta = \begin{bmatrix} \Delta^0 & \frac{\Delta^+}{\sqrt{2}} \\ \frac{\Delta^+}{\sqrt{2}} & \Delta^{++} \end{bmatrix} \tag{1}$$

with $L = 0$ and $L = -2$, respectively, and the scalar field σ with lepton number $L = 2$. Below we will consider the required vev hierarchies in the model.

2.1. Yukawa sector

Here we consider the simplest version of the seesaw scheme proposed in [14] in which no right-handed neutrinos are added, and only the $SU(3)_c \otimes SU(2)_L \otimes U(1)_Y$ electroweak breaking sector is extended so as to spontaneously break lepton number giving mass to neutrinos. Such '123' majoron–seesaw model is described by the $SU(3)_c \otimes SU(2)_L \otimes U(1)_Y \otimes U(1)_L$ invariant Yukawa Lagrangian,

$$\mathcal{L}_Y = y^d_{ij}\overline{Q}_i u_{R_j}\Phi + y^u_{ij}\overline{Q}_i d_{R_j}\tilde{\Phi} + y^\ell_{ij}\overline{L_i}\ell_{R_j}\Phi + y^\nu_{ij}L_i^T C\Delta L_j + \text{h.c.} \tag{2}$$

In this model the neutrino mass (see figure 1) is given by,

$$m_\nu = y^\nu \kappa v_1 \frac{v_2^2}{m_\Delta^2} \tag{3}$$

where v_1 and v_2 are the vevs of the singlet and the doublet, respectively. Here κ is a dimensionless parameter that describes the interaction amongst the three scalar fields (see below), and m_Δ is the mass of the scalar triplet Δ.

At this point we note that the smallness of neutrino mass i.e.

$$m_\nu \lesssim 1\ eV$$

may define interesting regions of the parameter space in any neutrino mass generation model where the new physics is expected to be hidden from direct observation. In particular, we are interested in spotting those regions accessible at collider searches such as the ongoing experiments at the LHC (see [20] and references therein).

In our pure type II seesaw model where lepton number is spontaneously violated at some low energy scale we have

$$m_\nu = y^\nu \langle \Delta \rangle$$

with the effective vev is given as $\langle \Delta \rangle = \mu \langle \Phi \rangle^2 / M_\Delta^2$ where Δ is the isotriplet lepton–number–carrying scalar. Here $\langle \Phi \rangle$ is fixed by the mass of the W boson and

$$\mu = \kappa v_1$$

is the dimensionful parameter responsible of lepton number violation, see equation (3). Therefore if $y^\nu \sim \mathcal{O}(1)$ and the mass M_Δ lies at 1 TeV region then one has that $\langle \Delta \rangle \sim m_\nu$ and $\mu \sim 1\ eV$.

Note that one may consider two situations: $v_1 \gg \Lambda_{EW}$ (high-scale seesaw mechanism) in whose case the scalar singlet and the invisible decays of the Higgs are decoupled [15]; the second interesting case is when $\Lambda_{EW} \lesssim v_1 \lesssim$ few TeV (low-scale seesaw mechanism). In this case the parameter κ is the range $[10^{-14},\ 10^{-16}]$ for $y^\nu \sim \mathcal{O}(1)$. In this case one has new physics at the TeV region including the 'invisible' decays of the Higgs Bosons.

Therefore, led by the smallness of the neutrino mass we can qualitatively determine that the analysis to be carried out is characterized by having a vev hierarchy

$$v_1 \gtrsim v_2 \gg v_3$$

and the smallness of the coupling κ, that is $\kappa \ll 1$.

2.2. The scalar potential

The scalar potential invariant under the $SU(3)_c \otimes SU(2)_L \otimes U(1)_Y \otimes U(1)_L$ symmetry is given by [15, 16] [5]

$$\begin{aligned} V = {} & \mu_1^2 \sigma^* \sigma + \mu_2^2 \Phi^\dagger \Phi + \mu_3^2 \mathrm{tr}(\Delta^\dagger \Delta) + \lambda_1 (\Phi^\dagger \Phi)^2 + \lambda_2 [\mathrm{tr}(\Delta^\dagger \Delta)]^2 \\ & + \lambda_3 \Phi^\dagger \Phi \mathrm{tr}(\Delta^\dagger \Delta) + \lambda_4 \mathrm{tr}(\Delta^\dagger \Delta \Delta^\dagger \Delta) + \lambda_5 (\Phi^\dagger \Delta^\dagger \Delta \Phi) + \beta_1 (\sigma^* \sigma)^2 \\ & + \beta_2 (\Phi^\dagger \Phi)(\sigma^* \sigma) + \beta_3 \mathrm{tr}(\Delta^\dagger \Delta)(\sigma^* \sigma) - \kappa (\Phi^T \Delta \Phi \sigma + \mathrm{h.c.}). \end{aligned} \tag{4}$$

As mentioned above the scalar fields σ, ϕ and Δ acquire non-zero vacuum expectation values, v_1, v_2 and v_3, respectively, so that, they can be shifted as follows,

$$\begin{aligned} \sigma &= \frac{v_1}{\sqrt{2}} + \frac{R_1 + iI_1}{\sqrt{2}}, \\ \phi^0 &= \frac{v_2}{\sqrt{2}} + \frac{R_2 + iI_2}{\sqrt{2}}, \\ \Delta^0 &= \frac{v_3}{\sqrt{2}} + \frac{R_3 + iI_3}{\sqrt{2}}. \end{aligned}$$

The minimization conditions of equation (4) are given by,

$$\begin{aligned} \mu_1^2 &= \frac{-2\beta_1 v_1^3 - \beta_2 v_1 v_2^2 - \beta_3 v_1 v_3^2 + \kappa v_2^2 v_3}{2v_1}, \\ \mu_2^2 &= -\frac{1}{2}(2\lambda_1 v_2^2 + \beta_2 v_1^2 + (\lambda_3 + \lambda_5) v_3^2 - 2\kappa v_1 v_3), \\ \mu_3^2 &= \frac{-2(\lambda_2 + \lambda_4) v_3^3 - (\lambda_3 + \lambda_5) v_2^2 v_3 - \beta_3 v_1^2 v_3 + \kappa v_1 v_2^2}{2v_3}. \end{aligned} \tag{5}$$

and from these one can derive a vev seesaw relation of the type

$$v_1 v_3 \sim \kappa v_2^2,$$

where κ is the dimensionless coupling that generates the mass parameter associated to the cubic term in the scalar potential of the simplest triplet seesaw scheme with explicit lepton number violationas proposed in [21] and recently revisited in [12].

Neutral Higgs Bosons

One can now write the resulting squared mass matrix for the CP-even scalars in the weak basis (R_1, R_2, R_3) as follows,

[5] From now on we follow the notation and conventions used in [16].

$$M_R^2 = \begin{bmatrix} 2\beta_1 v_1^2 + \frac{1}{2}\kappa v_2^2 \frac{v_3}{v_1} & \beta_2 v_1 v_2 - \kappa v_2 v_3 & \beta_3 v_1 v_3 - \frac{1}{2}\kappa v_2^2 \\ \beta_2 v_1 v_2 - \kappa v_2 v_3 & 2\lambda_1 v_2^2 & (\lambda_3 + \lambda_5) v_2 v_3 - \kappa v_1 v_2 \\ \beta_3 v_1 v_3 - \frac{1}{2}\kappa v_2^2 & (\lambda_3 + \lambda_5) v_2 v_3 - \kappa v_1 v_2 & 2(\lambda_2 + \lambda_4) v_3^2 + \frac{1}{2}\kappa v_2^2 \frac{v_1}{v_3} \end{bmatrix}. \quad (6)$$

The matrix M_R^2 is diagonalized by an orthogonal matrix as follows, $\mathcal{O}_R M_R^2 \mathcal{O}_R^T = \mathrm{diag}(m_{H_1}^2, m_{H_2}^2, m_{H_3}^2)$, where

$$\begin{pmatrix} H_1 \\ H_2 \\ H_3 \end{pmatrix} = \mathcal{O}_R \begin{pmatrix} R_1 \\ R_2 \\ R_3 \end{pmatrix}. \quad (7)$$

We use the standard parameterization $\mathcal{O}_R = R_{23} R_{13} R_{12}$ where

$$R_{12} = \begin{pmatrix} c_{12} & s_{12} & 0 \\ -s_{12} & c_{12} & 0 \\ 0 & 0 & 1 \end{pmatrix}, \quad R_{13} = \begin{pmatrix} c_{13} & 0 & s_{13} \\ 0 & 1 & 0 \\ -s_{13} & 0 & c_{13} \end{pmatrix}, \quad R_{23} = \begin{pmatrix} 1 & 0 & 0 \\ 0 & c_{23} & s_{23} \\ 0 & -s_{23} & c_{23} \end{pmatrix} \quad (8)$$

and $c_{ij} = \cos\alpha_{ij}$, $s_{ij} = \sin\alpha_{ij}$, so that the rotation matrix $\mathcal{O}_R$ is re-expressed in terms of the mixing angles in the following way:

$$\mathcal{O}_R = \begin{pmatrix} c_{12}c_{13} & c_{13}s_{12} & s_{13} \\ -c_{23}s_{12} - c_{12}s_{13}s_{23} & c_{23}c_{12} - s_{12}s_{13}s_{23} & c_{13}s_{23} \\ -c_{12}c_{23}s_{13} + s_{23}s_{12} & -c_{23}s_{12}s_{13} - c_{12}s_{23} & c_{13}c_{23} \end{pmatrix}. \quad (9)$$

On the other hand, the squared mass matrix for the CP-odd scalars in the weak basis (I_1, I_2, I_3) is given as,

$$M_I^2 = \kappa \begin{bmatrix} \frac{1}{2} v_2^2 \frac{v_3}{v_1} & v_2 v_3 & \frac{1}{2} v_2^2 \\ v_2 v_3 & 2 v_1 v_3 & v_1 v_2 \\ \frac{1}{2} v_2^2 & v_1 v_2 & \frac{1}{2} v_2^2 \frac{v_1}{v_3} \end{bmatrix}. \quad (10)$$

The matrix M_I^2 is diagonalized as, $\mathcal{O}_I M_I^2 \mathcal{O}_I^T = \mathrm{diag}(0, 0, m_A^2)$, where the null masses correspond to the would-be Goldstone boson G^0 and the Majoron J, while the squared CP-odd mass is

$$m_A^2 = \kappa \left(\frac{v_2^2 v_1^2 + v_2^2 v_3^2 + 4 v_3^2 v_1^2}{2 v_3 v_1} \right). \quad (11)$$

The mass eigenstates are linked with the original ones by the following rotation,

$$\begin{pmatrix} A_1 \\ A_2 \\ A_3 \end{pmatrix} \equiv \begin{pmatrix} J \\ G^0 \\ A \end{pmatrix} = \mathcal{O}_I \begin{pmatrix} I_1 \\ I_2 \\ I_3 \end{pmatrix} \quad (12)$$

where the matrix $\mathcal{O}_I$ is given by,

$$O_I = \begin{bmatrix} c v_1 V^2 & -2 c v_2 v_3^2 & -c v_2^2 v_3 \\ 0 & v_2/V & -2 v_3/V \\ b v_2/2 v_1 & b & b v_2/2 v_3 \end{bmatrix}, \quad (13)$$

with

$$V^2 = v_2^2 + 4 v_3^2,$$
$$c^{-2} = v_1^2 V^4 + 4 v_2^2 v_3^4 + v_2^4 v_3^2 \quad (14)$$

$$b^2 = \frac{4 v_1^2 v_3^2}{v_2^2 v_1^2 + v_2^2 v_3^2 + 4 v_3^2 v_1^2}. \quad (15)$$

Charged Higgs Bosons

The squared mass matrix for the singly-charged scalar bosons in the original weak basis ($\phi^{\pm}$, $\Delta^{\pm}$) is given by,

$$M^2_{H^{\pm}} = \begin{bmatrix} \kappa v_1 v_3 - \frac{1}{2}\lambda_5 v_3^2 & \frac{1}{2\sqrt{2}} v_2(\lambda_5 v_3 - 2\kappa v_1) \\ \frac{1}{2\sqrt{2}} v_2(\lambda_5 v_3 - 2\kappa v_1) & \frac{1}{4v_3} v_2^2(-\lambda_5 v_3 + 2\kappa v_1) \end{bmatrix}. \tag{16}$$

We now define

$$\begin{pmatrix} G^{\pm} \\ H^{\pm} \end{pmatrix} = \begin{pmatrix} c_{\pm} & s_{\pm} \\ -s_{\pm} & c_{\pm} \end{pmatrix} \begin{pmatrix} \phi^{\pm} \\ \Delta^{\pm} \end{pmatrix}, \quad \text{and} \quad \mathcal{O}_{\pm} M^2_{H^{\pm}} \mathcal{O}^T_{\pm} = \text{diag}(0,\, m^2_{H^{\pm}}). \tag{17}$$

where $c_{\pm}$ and $s_{\pm}$ are given as $c_{\pm} = v_2/\sqrt{v_2^2 + 2v_3^2}$ and $s_{\pm} = \sqrt{2}\, v_3/\sqrt{v_2^2 + 2v_3^2}$. The massless state corresponds to the would-be Golstone bosons $G^{\pm}$ and the massive state $H^{\pm}$ is characterized by,

$$m^2_{H^{\pm}} = \frac{1}{4v_3}(2\kappa v_1 - \lambda_5 v_3)(v_2^2 + 2v_3^2). \tag{18}$$

On the other hand, the doubly-charged scalars $\Delta^{\pm\pm}$ has mass

$$m^2_{\Delta^{++}} = \frac{1}{2v_3}(\kappa v_1 v_2^2 - 2\lambda_4 v_3^3 - \lambda_5 v_2^2 v_3). \tag{19}$$

2.3. Scalar boson mass sum rules

Notice that using the fact that the smallness of the neutrino mass implies that the parameters κ and v_3 are very small one can, to a good approximation, rewrite equation (6) schematically in the form,

$$M_R^2 \sim \begin{pmatrix} \star & \star & 0 \\ \star & \star & 0 \\ 0 & 0 & \star \end{pmatrix} \text{ so that } \mathcal{O}_R \sim \begin{pmatrix} c_{12} & s_{12} & 0 \\ -s_{12} & c_{12} & 0 \\ 0 & 0 & 1 \end{pmatrix}, \tag{20}$$

and equation (11) becomes,

$$m_A^2 \sim \kappa \frac{v_2^2 v_1}{2v_3}. \tag{21}$$

As a result, the scalar H_3 and the pseudo-scalar A are almost degenerate,

$$m_{H_3} = (M_R^2)_{33} \approx m_A^2. \tag{22}$$

In the same way, by using equations (11), (18) and (19), one can derive the following mass relations,

$$m_A^2 - m^2_{H^+} \approx \frac{\lambda_5 v_2^2}{4} \quad \text{and} \quad 2m^2_{H^+} - m_A^2 - m^2_{\Delta^{++}} \approx \lambda_4 v_3^2,$$

which can be rewritten in the form,

$$m^2_{H^+} - m^2_{\Delta^{++}} \approx m_A^2 - m^2_{H^+} \approx \frac{\lambda_5 v_2^2}{4}. \tag{23}$$

This sum rule is also satisfied in the type-II seesaw model with explicit breaking of lepton number. Imposing the perturbativity condition one finds that the squared mass difference between, say doubly and singly charged scalar bosons, cannot be too large [12]. Explicit comparison shows that λ_5 in equation (4) corresponds to $\lambda'_{H\Delta}$ in [12]. Therefore when the couplings of the singlet σ in equation (4) are small, λ_5 is constrained to be in the range $[-0.85,\ 0.85]$, so that the remaining couplings are kept small up to the Planck scale and vacuum stability is guaranteed. See figure 4 in [12]. Likewise when one decouples the triplet one also recovers the results found in [11].

3. Theoretical constraints

Before analyzing the sensitivities of the searches for Higgs Bosons at the LHC experiments, we first discuss the restrictions that follow from the consistency requirements of the Higgs potential. We can rewrite the dimensionless parameters $\lambda_{1,2,3}$ and $\beta_{1,2,3}$ in equation (4) in terms of the mixing angles, α_{ij} and scalar the masses $m_{H_{1,2,3}}$ by solving $\mathcal{O}_R M_R^2 \mathcal{O}_R^T = \text{diag}(m^2_{H_1},\, m^2_{H_2},\, m^2_{H_3})$ and $\mathcal{O}_I M_I^2 \mathcal{O}_I^T = \text{diag}(0,\, 0,\, m_A^2)$. Hence one gets,

$$\lambda_1 = \frac{1}{2v_2^2}[m_{H_1}^2 c_{13}^2 s_{12}^2 + m_{H_2}^2 (c_{12}c_{23} - s_{12}s_{13}s_{23})^2 + m_{H_3}^2 (c_{12}s_{23} + s_{12}s_{13}c_{23})^2]$$

$$\lambda_2 = \frac{1}{2v_3^2}[m_{H_1}^2 s_{13}^2 + c_{13}^2 (m_{H_2}^2 s_{23}^2 + m_{H_3}^2 c_{23}^2)] - \left(\lambda_4 + \kappa\frac{v_1 v_2^2}{4v_3^3}\right)$$

$$\lambda_3 = \frac{c_{13}}{v_2 v_3}[m_{H_1}^2 s_{12}s_{13} + m_{H_2}^2 s_{23}(c_{12}c_{23} - s_{12}s_{13}s_{23}) - m_{H_3}^2 c_{23}(c_{12}s_{23} + s_{12}s_{13}c_{23})] - \left(\lambda_5 - \kappa\frac{v_1}{v_3}\right)$$

$$\beta_1 = \frac{1}{2v_1^2}[m_{H_1}^2 c_{12}^2 c_{13}^2 + m_{H_2}^2 (s_{12}c_{23} + c_{12}s_{23}s_{13})^2 + m_{H_3}^2 (s_{12}s_{23} - c_{12}c_{23}s_{13})^2] - \kappa\frac{v_2^2 v_3}{4v_1^3}$$

$$\beta_2 = \frac{1}{v_1 v_2}[m_{H_1}^2 c_{12}s_{12}c_{13}^2 - m_{H_2}^2 (c_{23}s_{12} + c_{12}s_{13}s_{23})(c_{12}c_{23} - s_{12}s_{13}s_{23}) - m_{H_3}^2 (s_{23}s_{12} - c_{12}s_{13}c_{23})(c_{12}s_{23} + s_{12}s_{13}c_{23})] + \kappa\frac{v_3}{v_1}$$

$$\beta_3 = \frac{c_{13}}{v_1 v_3}[m_{H_1}^2 c_{12}s_{13} - m_{H_2}^2 s_{23}(s_{12}c_{23} + c_{12}s_{13}s_{23}) + m_{H_3}^2 c_{23}(s_{12}s_{23} - c_{12}s_{13}c_{23})] + \kappa\frac{v_2^2}{2v_1 v_3}.$$

In addition, using equations (11), (18) and (19) we can write the dimensionless parameters $\lambda_{4,5}$ and κ as functions of the vevs $v_{1,2,3}$ and the masses of the pseudo-, singly- and doubly-charged scalar bosons (i.e. m_A, $m_{H^\pm}$ and $m_{\Delta^{\pm\pm}}$, respectively) as,

$$\lambda_4 = \frac{1}{v_3^2}\left(2m_{H^\pm}^2\frac{v_2^2}{v_2^2 + 2v_3^2} - m_A^2\frac{v_1^2 v_2^2}{v_2^2 v_3^2 + v_1^2(v_2^2 + 4v_3^2)} - m_{\Delta^{\pm\pm}}^2\right)$$

$$\lambda_5 = \left(-4m_{H^\pm}^2\frac{1}{v_2^2 + 2v_3^2} + 4m_A^2\frac{v_1^2}{v_2^2 v_3^2 + v_1^2(v_2^2 + 4v_3^2)}\right)$$

$$\kappa = 2m_A^2\frac{v_1 v_3}{v_2^2 v_3^2 + v_1^2(v_2^2 + 4v_3^2)}. \tag{24}$$

From the theoretical side we have to ensure that the scalar potential in the model is bounded from below (BFB).

3.1. Boundedness conditions

In order to ensure that the scalar potential in equation (4) is bounded from below we have to derive the conditions on the dimensionless parameters such the quartic part of the scalar potential is positive $V^{(4)} > 0$ as the fields go to infinity. We have that the parameter $\kappa \ll 1$ (due to the smallness of the neutrino mass) and non-negative. This follows from

$$\kappa \approx 2m_A^2\frac{v_3}{v_1 v_2^2}. \tag{25}$$

where we have used the last expression in equation (24) and the fact that $v_3 \ll v_2,\ v_1$. Then κ is neglected with respect to the other dimensionless parameters λ_i and β_j, i.e. $\lambda_i,\ \beta_j \gg \kappa$. As a result the quartic part of the potential $V^{(4)}|_{\kappa=0}$ turns to be a biquadratic form $\lambda_{ij}\varphi_i^2\varphi_j^2$ of real fields. Therefore, in this strict limit, the copositivity criteria described in [22] may be applied and the boundedness conditions for equation (4) are the following,

$$\lambda_1 > 0,\ \ \beta_1 > 0,\ \ \lambda_{24} > 0,\ \ \hat{\lambda} \equiv \beta_2 + 2\sqrt{\beta_1\lambda_1} > 0,$$
$$\tilde{\lambda} \equiv \beta_3 + 2\sqrt{\beta_1\lambda_{24}} > 0,\ \ \bar{\lambda} \equiv \lambda_3 + \theta(-\lambda_5)\lambda_5 + 2\sqrt{\lambda_1\lambda_{24}} > 0,\ \text{and}$$
$$\sqrt{\beta_1\lambda_1\lambda_{24}} + [\lambda_3 + \theta(-\lambda_5)\lambda_5]\sqrt{\beta_1} + \beta_2\sqrt{\lambda_{24}} + \beta_3\sqrt{\lambda_1} + \sqrt{\hat{\lambda}\tilde{\lambda}\bar{\lambda}} > 0, \tag{26}$$

where $\lambda_{24} \equiv \lambda_2 + \lambda_4$. In addition all the dimensionless parameters in the scalar potential are required to be less than $\sqrt{4\pi}$ in order to fulfill the perturbativity condition.

3.2. Astrophysical constraints

In our type-II seesaw model there are some constraints on the magnitude of $SU(2)$ triplet's vev $\langle\Delta\rangle = v_3$, that one must take into account. First of all, v_3 is constrained to be smaller than a few GeVs due to the ρ parameter ($\rho = 1.0004 \pm 0.00024$ [23]).

On the other hand, the presence of the Nambu-Goldstone boson associated to spontaneous lepton number violationand neutrino mass generation implies that there is a most stringent constraint on v_3 coming from

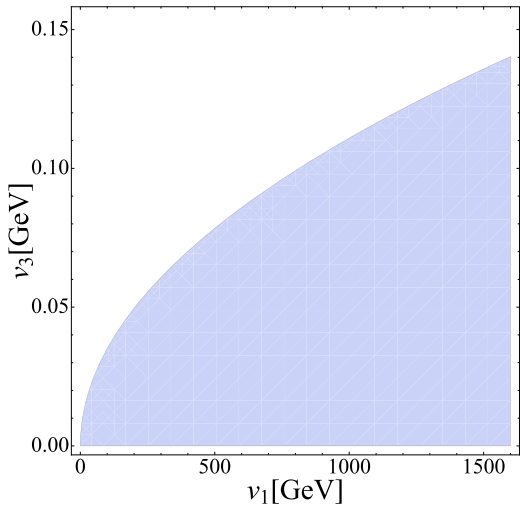

Figure 2. The shaded region represents the allowed region of v_3 as function of v_1.

astrophysics, due to supernova cooling. If the majoron is a strict Goldstone boson (or lighter than typical stellar temperatures) one has an upper bound for the Majoron-electron coupling

$$|g_{Jee}| \lesssim 10^{-13},$$

This is discussed, for example, in [24] and references therein. This implies

$$|g_{Jee}| = |\mathcal{O}^I_{12} m_e / v_2|.$$

Taking into account the profile of the Majoron [14][6] one can translate this as a bound on the projection of the Majoron onto the doublet as follows [16]

$$|\langle J|\phi\rangle| = \frac{2|v_2|v_3^2}{\sqrt{v_1^2\,(v_2^2 + 4v_3^2)^2 + 4v_2^2 v_3^4 + v_2^4 v_3^2}} \lesssim 10^{-7}. \tag{27}$$

Notice that this restriction on the triplet's vev is stronger that the one stemming from the ρ parameter. The shaded region in figure 2 corresponds to the allowed region of v_3 as function of v_1.

To close this section we mention that our phenomenological analysis remains valid if the Nambu-Goldstone boson picks up a small mass from, say, quantum gravity effects.

4. Type-II seesaw Higgs searches at the LHC

We now turn to the study of the experimental sensitivities of the LHC experiments to the parameters characterizing the '123' type-II majoron seesaw Higgs sector, as proposed in [14]. In the following we will assume that $m_{H_1} < m_{H_2} < m_{H_3}$ where 1, 2, 3 refer to the mass ordering in the CP even Higgs sector. Therefore, there are two possible cases that can be considered[7]:

i. $m_{H_1} < m_H$ and $m_{H_2} = m_H$;

ii. $m_{H_1} = m_H$,

where m_H is the mass of the Higgs reported by the ATLAS [2] and CMS [25] collaborations, i.e. $m_H = 125.09 \pm 0.21\,(\text{stat.}) \pm 0.11\,(\text{syst.})$ GeV [26]. For case (i), we have to enforce the constraints coming from LEP-II data on the lightest CP-even scalar coupling to the SM and those coming from the LHC Run-1 on the heavier scalars. Such situation has been discussed by us in [13] in the simplest '12-type' seesaw Majoron model. In case (ii), only the constraints coming from the LHC must be taken into account.

[6] This is derived either by explicit analysis of the scalar potential or simply by symmetry, using Noether's theorem [14].

[7] Recall that $m_{H_3} \approx m_A$, equation (22), which implies that the mass of H_3 must be close to that of the doubly-charged scalar mass. Therefore, as we will see in the next section, the existing bounds on searches of the doubly-charged scalar exclude the case where m_{H_3} is lighter than the other CP-even mass eigenstates.

Table 1. Current experimental results of ATLAS and CMS, [28].

channel	ATLAS	CMS	ATLAS+CMS
$\mu_{\gamma\gamma}$	$1.15^{+0.27}_{-0.25}$	$1.12^{+0.25}_{-0.23}$	$1.16^{+0.20}_{-0.18}$
μ_{WW}	$1.23^{+0.23}_{-0.21}$	$0.91^{+0.24}_{-0.21}$	$1.11^{+0.18}_{-0.17}$
μ_{ZZ}	$1.51^{+0.39}_{-0.34}$	$1.05^{+0.32}_{-0.27}$	$1.31^{+0.27}_{-0.24}$
$\mu_{\tau\tau}$	$1.41^{+0.40}_{-0.35}$	$0.89^{+0.31}_{-0.28}$	$1.12^{+0.25}_{-0.23}$
μ_{bb}	$0.62^{+0.37}_{-0.36}$	$0.81^{+0.45}_{-0.42}$	$0.69^{+0.29}_{-0.27}$

Table 2. Scalar mass eigenstates in the model. $c_\pm = v_2/\sqrt{v_2^2+2v_3^2}$, $s_\pm = \sqrt{2}\,v_3/\sqrt{v_2^2+2v_3^2}$.

Mass eigenstate ϕ	Mass squared m_ϕ^2	Composition
H_i $(i = 1, 2, 3)$	m_i^2	$\mathcal{O}^R_{i1}R_1 + \mathcal{O}^R_{i2}R_2 + \mathcal{O}^R_{i3}R_3$
J	0	$\mathcal{O}^I_{11}I_1 + \mathcal{O}^I_{12}I_2 + \mathcal{O}^I_{13}I_3$
G^0	0	$\mathcal{O}^I_{22}I_2 + \mathcal{O}^I_{23}I_3$
A	$\kappa\left(\frac{v_2^2v_1^2+v_2^2v_3^2+4v_3^2v_1^2}{2v_3v_1}\right)$	$\mathcal{O}^I_{31}I_1 + \mathcal{O}^I_{32}I_2 + \mathcal{O}^I_{33}I_3$
$G^\pm$	0	$c_\pm\phi^\pm + s_\pm\Delta^\pm$
$H^\pm$	$\frac{1}{4v_3}(2\kappa v_1 - \lambda_5 v_3)(v_2^2+2v_3^2)$	$-s_\pm\phi^\pm + c_\pm\Delta^\pm$
$\Delta^{\pm\pm}$	$\frac{1}{2v_3}(\kappa v_1 v_2^2 - 2\lambda_4 v_3^3 - \lambda_5 v_2^2 v_3)$	$\Delta^{\pm\pm}$

The neutral component of the Standard Model Higgs doublet couplings get modified as follows,

$$\phi^0 \to C_1H_1 + C_2H_2 + C_3H_3 \tag{28}$$

where we have defined $C_i \equiv \mathcal{O}^R_{i2}$ and $\mathcal{O}^R_{ij}$ are the matrix elements of $\mathcal{O}^R$ in equation (9).

4.1. LEP constraints on invisible Higgs decays

The constraints on H_1, when $m_{H_1} < 125$ GeV, stem from the process $e^+e^- \to Zh \to Zb\bar{b}$ which is written as [27]

$$\begin{aligned}\sigma_{hZ\to b\bar{b}Z} &= \sigma^{SM}_{hZ} \times R_{hZ} \times BR(h \to b\bar{b}) \\ &= \sigma^{SM}_{hZ} \times C^2_{Z\,(h\to b\bar{b})},\end{aligned} \tag{29}$$

where σ^{SM}_{hZ} is the SM hZ cross section, R_{hZ} is the suppression factor related to the coupling of the Higgs Boson[8] to the gauge boson Z. Since $v_3 \ll v_2$, we have that the factor $R_{H_iZ} \approx C_i^2$ where $C_1 = \cos\alpha_{13}\sin\alpha_{12}$, equation (28). Notice that $C_1 \approx \sin\alpha_{12}$ for the limit $\alpha_{13} \ll 1$ and then one obtains the same exclusion region depicted in figure 1 in [13].

4.2. LHC constraints on the Higgs signal strengths

In addition, we have to enforce the limits coming from the Standard Modeldecay channels of the Higgs Boson. These are given in terms of the signal strength parameters,

$$\mu_f = \frac{\sigma^{\mathrm{NP}}(pp \to h)}{\sigma^{\mathrm{SM}}(pp \to h)}\,\frac{BR^{\mathrm{NP}}(h \to f)}{BR^{\mathrm{SM}}(h \to f)}, \tag{30}$$

where σ is the cross section for Higgs production, $BR\,(h \to f)$ is the branching ratio into the Standard Modelfinal state f, the labels NP and SM stand for New Physics and Standard Model, respectively. These can be compared with those given by the experimental collaborations. The most recent results of the signal strengths from a combined ATLAS and CMS analysis [28] are shown in table 1.

One can see with ease that the LHC results indicate that $\mu_{VV} \sim 1$. In our analysis, we assume that the LHC allows deviations up to 20% as follows,

$$0.8 \leqslant \mu_{XX} \leqslant 1.2 \tag{31}$$

[8] The Feynman rules for the couplings of the Higgs Bosons H_i to the Z are the following: $i\frac{g^2}{2c_W^2}(\mathcal{O}^R_{i2}v_2 + \mathcal{O}^R_{i3}v_3)g_{\mu\nu}$.

4.3. LHC bounds on the heavy neutral scalars

In our study we will impose the constraints on the heavy scalars from the recent LHC scalar boson searches. Therefore, we use the bounds set by the search for a heavy Higgs in the $H \to WW$ and $H \to ZZ$ decay channels in the range [145−1000] GeV [29] and in the $h \to \tau\tau$ decay channel in the range range [100−1000] GeV [30]. We also adopt the constraints on the process $h \to \gamma\gamma$ in the range [65−600] GeV [31] and the range [150, 850] GeV [32]. Besides, we impose the bounds in the $A \to Zh$ decay channel in the range [220−1000] GeV [33].

4.4. Summary of the searches of charged scalars

The type-II seesaw model with explicit breaking of lepton number contains seven physical scalars: two CP-even neutral scalars H_1 and H_2, one CP-odd scalar A and four charged scalars $\Delta^{\pm\pm}$ and $H^{\pm}$. Such a scenario has been widely studied in the literature and turns out to be quite appealing because it could be tested at the LHC [34–44]. For instance, the existence of charged scalar bosons provides additional contributions to the one-loop decays of the Standard Model Higgs Boson. Indeed, they could affect the one-loop decays $h \to \gamma\gamma$ [39, 40] and $h \to Z\gamma$ [40] in a substantial way. In this case the signal strength $\mu_{\gamma\gamma}$ can set bounds on the mass of the charged scalars, $\Delta^{\pm\pm}$ and/or $H^{\pm}$.

The doubly-charged scalar boson has the following possible decay channels: $\ell^{\pm}\ell^{\pm}$, $W^{\pm}W^{\pm}$, $W^{\pm}H^{\pm}$ and $H^{\pm}H^{\pm}$. However, it is known that for an approximately degenerate triplet mass spectrum and vev $v_3 \lesssim 10^{-4}$ GeV the doubly charged Higgs coupling to $W^{\pm}$ is suppressed (because it is proportional to v_3 as can be seen from table 3) and hence $\Delta^{\pm\pm}$ predominantly decays into like-sign dileptons [41, 44, 45]. In this case, CMS [46] and ATLAS [47] have currently excluded at 95% C.L., depending on the assumptions on the branching ratios into like-sign dileptons, doubly-charged masses between 200 and 460 GeV[9]. For $v_3 \gtrsim 10^{-4}$ GeV, the Yukawa couplings of triplet to leptons are too small so that $\Delta^{\pm\pm}$ dominantly decays to like-sign dibosons, in which case the collider limits are rather weak [43, 48–50].

In the present '123' type-II seesaw model there are two additional physical scalars, a massive CP-even scalar H_3 and the massless majoron J. The latter, associated to the spontaneous breaking of lepton number, provides non-standard decay channels of other Higgs Bosons as missing energy in the final state[10].

5. Invisible Higgs decays at the LHC

We now turn to the case of genuinely non-standard Higgs decays. We focus on investigating the LHC sensitivities on the invisible Higgs decays. In so doing we take into account how they are constrained by the available experimental data. In the previous section we mentioned that in our study the CP- even scalars obey the following mass hierarchy $m_{H_1} < m_{H_2} < m_{H_3}$. Furthermore, we will also assume that the masses m_{H_3}, m_A, m_{H^+} and $m_{\Delta^{++}}$ are nearly degenerate.

As a consequence, the decay of any CP-even Higgs H_i into the pseudo-scalar A is not kinematically allowed. Therefore, the new decay channels of the CP-even scalars are just, $H_i \to JJ$ and $H_i \to 2H_j$ (when $m_{H_i} < \frac{m_{H_j}}{2}$ for $i \neq j$). The latter contributing also to the invisible decay channel of the Higgs as, $H_i \to 2H_j \to 4J$.

The Higgs-Majoron couplings are given by,

$$g_{H_aJJ} = \left(\frac{(\mathcal{O}^I_{12})^2}{v_2}\mathcal{O}^R_{a2} + \frac{(\mathcal{O}^I_{13})^2}{v_3}\mathcal{O}^R_{a3} + \frac{(\mathcal{O}^I_{11})^2}{v_1}\mathcal{O}^R_{a1} \right) m^2_{H_a}, \tag{32}$$

where $\mathcal{O}^I_{ij}$ are the elements of the rotation matrix in equation (13) and the decay width is given by

$$\Gamma(H_a \to JJ) = \frac{1}{32\pi}\frac{g^2_{H_aJJ}}{m_{H_a}}. \tag{33}$$

[9] From doubly-charged scalar boson searches performed by ATLAS and CMS one can also constrain the lepton number violation processes $pp \to \Delta^{\pm\pm}\Delta^{\mp\mp} \to \ell^{\pm}\ell^{\pm}W^{\mp}W^{\mp}$ and $pp \to \Delta^{\pm\pm}H^{\mp} \to \ell^{\pm}\ell^{\pm}W^{\mp}Z$ [41]. This may also shed light on the Majorana phases of the lepton mixing matrix [34–36].

[10] These include, for example, $H_i \to JJ$ and $H^{\pm} \to JW^{\mp}$. Here we focus mainly on the first, the decays of $H^{\pm}$ deserve further study but it is beyond the scope of this work and will be considered elsewhere.

Table 3. Feynman rules for the couplings of the Higgs Bosons H_i to the gauge bosons.

	Vertex	Gauge Coupling
1	$H_1 W_\mu^+ W_\nu^-$	$i\frac{g^2}{2}(\mathcal{O}_{12}^R v_2 + 2\mathcal{O}_{13}^R v_3)\, g_{\mu\nu}$
2	$H_2 W_\mu^+ W_\nu^-$	$i\frac{g^2}{2}(\mathcal{O}_{22}^R v_2 + 2\mathcal{O}_{23}^R v_3)\, g_{\mu\nu}$
3	$H_3 W_\mu^+ W_\nu^-$	$i\frac{g^2}{2}(\mathcal{O}_{32}^R v_2 + 2\mathcal{O}_{33}^R v_3)\, g_{\mu\nu}$
4	$\Delta^{\pm\pm} W_\mu^\mp W_\nu^\mp$	$i2g^2\frac{v_3}{\sqrt{2}} g_{\mu\nu}$
5	$H^\pm W_\mu^\mp Z_\nu$	$i\frac{g^2}{c_W}\frac{c_\pm v_3}{\sqrt{2}} g_{\mu\nu}$
6	$G^\pm W_\mu^\mp Z_\nu$	$i\frac{g^2}{c_W}\left(\frac{v_2}{2}s_W^2 c_\pm + \frac{v_3}{\sqrt{2}}(1+s_W^2)s_\pm\right) g_{\mu\nu}$
7	$G^\pm W_\mu^\mp A_\nu$	$-iem_W g_{\mu\nu}$
8	$\Delta^{++}\Delta^{--} W_\mu^+ W_\nu^-$	$ig^2\, g_{\mu\nu}$
9	$H^+H^- W_\mu^+ W_\nu^-$	$i\frac{g^2}{2}(1+3c_\pm^2)\, g_{\mu\nu}$
10	$G^+G^- W_\mu^+ W_\nu^-$	$i\frac{g^2}{2}(1+3s_\pm^2)\, g_{\mu\nu}$
11	$H_1H_1 W_\mu^+ W_\nu^-$	$i\frac{g^2}{2}(\mathcal{O}_{12}^{R\,2} + 2\mathcal{O}_{13}^{R\,2})\, g_{\mu\nu}$
12	$H_2H_2 W_\mu^+ W_\nu^-$	$i\frac{g^2}{2}(\mathcal{O}_{22}^{R\,2} + 2\mathcal{O}_{23}^{R\,2})\, g_{\mu\nu}$
13	$H_3H_3 W_\mu^+ W_\nu^-$	$i\frac{g^2}{2}(\mathcal{O}_{32}^{R\,2} + 2\mathcal{O}_{33}^{R\,2})\, g_{\mu\nu}$
14	$JJ W_\mu^+ W_\nu^-$	$i\frac{g^2}{2}(\mathcal{O}_{12}^{I\,2} + 2\mathcal{O}_{13}^{I\,2})\, g_{\mu\nu}$
15	$G^0G^0 W_\mu^+ W_\nu^-$	$i\frac{g^2}{2}(\mathcal{O}_{22}^{I\,2} + 2\mathcal{O}_{23}^{I\,2})\, g_{\mu\nu}$
16	$AA W_\mu^+ W_\nu^-$	$i\frac{g^2}{2}(\mathcal{O}_{32}^{I\,2} + 2\mathcal{O}_{33}^{I\,2})\, g_{\mu\nu}$
17	$\Delta^{\pm\pm} H^\mp W_\nu^\mp$	$\mp igc_\pm\, (p_1-p_2)_\mu$
18	$\Delta^{\pm\pm} G^\mp W_\nu^\mp$	$\mp igs_\pm\, (p_1-p_2)_\mu$
19	$H_1 H^\pm W_\mu^\mp$	$\pm i\frac{g}{2}(s_\pm\mathcal{O}_{12}^R - \sqrt{2}\,c_\pm\mathcal{O}_{13}^R)\, (p_1-p_2)_\mu$
20	$H_2 H^\pm W_\mu^\mp$	$\pm i\frac{g}{2}(s_\pm\mathcal{O}_{22}^R - \sqrt{2}\,c_\pm\mathcal{O}_{23}^R)\, (p_1-p_2)_\mu$
21	$H_3 H^\pm W_\mu^\mp$	$\pm i\frac{g}{2}(s_\pm\mathcal{O}_{32}^R - \sqrt{2}\,c_\pm\mathcal{O}_{33}^R)\, (p_1-p_2)_\mu$
22	$H^\pm J W_\mu^\mp$	$\frac{g}{2}(s_\pm\mathcal{O}_{12}^I + \sqrt{2}\,c_\pm\mathcal{O}_{13}^I)\, (p_1-p_2)_\mu$
23	$G^0 H^\pm W_\mu^\mp$	$-\frac{g}{2}(s_\pm\mathcal{O}_{22}^I + \sqrt{2}\,c_\pm\mathcal{O}_{23}^I)\, (p_1-p_2)_\mu$
24	$A H^\pm W_\mu^\mp$	$-\frac{g}{2}(s_\pm\mathcal{O}_{32}^I + \sqrt{2}\,c_\pm\mathcal{O}_{33}^I)\, (p_1-p_2)_\mu$
25	$G^\pm H_1 W_\mu^\mp$	$\pm i\frac{g}{2}(c_\pm\mathcal{O}_{12}^R + \sqrt{2}\,s_\pm\mathcal{O}_{13}^R)\, (p_1-p_2)_\mu$
26	$G^\pm H_2 W_\mu^\mp$	$\pm i\frac{g}{2}(c_\pm\mathcal{O}_{22}^R + \sqrt{2}\,s_\pm\mathcal{O}_{23}^R)\, (p_1-p_2)_\mu$
27	$G^\pm H_3 W_\mu^\mp$	$\pm i\frac{g}{2}(c_\pm\mathcal{O}_{32}^R + \sqrt{2}\,s_\pm\mathcal{O}_{33}^R)\, (p_1-p_2)_\mu$
28	$G^\pm J W_\mu^\mp$	$-\frac{g}{2}(c_\pm\mathcal{O}_{12}^I - \sqrt{2}\,s_\pm\mathcal{O}_{13}^I)\, (p_1-p_2)_\mu$
29	$G^0 G^\pm W_\mu^-$	$\frac{g}{2}(c_\pm\mathcal{O}_{22}^I - \sqrt{2}\,s_\pm\mathcal{O}_{23}^I)\, (p_1-p_2)_\mu$

Table 3. (Continued.)

	Vertex	Gauge Coupling
30	$AG^{\pm}W_{\mu}^{-}$	$\frac{g}{2}(c_{\pm}\mathcal{O}_{32}^{I}-\sqrt{2}\,s_{\pm}\mathcal{O}_{33}^{I})\,(p_1-p_2)_{\mu}$
	Vertex	Gauge Coupling
31	$H_1Z_{\mu}Z_{\nu}$	$i\frac{g^2}{2c_W^2}(\mathcal{O}_{12}^{R}v_2+4\mathcal{O}_{13}^{R}v_3)\,g_{\mu\nu}$
32	$H_2Z_{\mu}Z_{\nu}$	$i\frac{g^2}{2c_W^2}(\mathcal{O}_{22}^{R}v_2+4\mathcal{O}_{23}^{R}v_3)\,g_{\mu\nu}$
33	$H_3Z_{\mu}Z_{\nu}$	$i\frac{g^2}{2c_W^2}(\mathcal{O}_{32}^{R}v_2+4\mathcal{O}_{33}^{R}v_3)\,g_{\mu\nu}$
34	$\Delta^{++}\Delta^{--}Z_{\mu}Z_{\nu}$	$i\frac{2g^2}{c_W^2}(c_W^2-s_W^2)^2\,g_{\mu\nu}$
35	$H^{+}H^{-}Z_{\mu}Z_{\nu}$	$i\frac{g^2}{2c_W^2}(s_{\pm}^2(c_W^2-s_W^2)^2+4s_W^4c_{\pm}^2)\,g_{\mu\nu}$
36	$G^{+}G^{-}Z_{\mu}Z_{\nu}$	$i\frac{g^2}{2c_W^2}(c_{\pm}^2(c_W^2-s_W^2)^2+4s_W^4s_{\pm}^2)\,g_{\mu\nu}$
37	$H_1H_1Z_{\mu}Z_{\nu}$	$i\frac{g^2}{2c_W^2}(\mathcal{O}_{12}^{R\,2}+4\mathcal{O}_{13}^{R\,2})\,g_{\mu\nu}$
38	$H_2H_2Z_{\mu}Z_{\nu}$	$i\frac{g^2}{2c_W^2}(\mathcal{O}_{22}^{R\,2}+4\mathcal{O}_{23}^{R\,2})\,g_{\mu\nu}$
39	$H_3H_3Z_{\mu}Z_{\nu}$	$i\frac{g^2}{2c_W^2}(\mathcal{O}_{32}^{R\,2}+4\mathcal{O}_{33}^{R\,2})\,g_{\mu\nu}$
40	$JJZ_{\mu}Z_{\nu}$	$i\frac{g^2}{2c_W^2}(\mathcal{O}_{12}^{I\,2}+4\mathcal{O}_{13}^{I\,2})\,g_{\mu\nu}$
41	$G^0G^0Z_{\mu}Z_{\nu}$	$i\frac{g^2}{2c_W^2}(\mathcal{O}_{22}^{I\,2}+4\mathcal{O}_{23}^{I\,2})\,g_{\mu\nu}$
42	$AAZ_{\mu}Z_{\nu}$	$i\frac{g^2}{2c_W^2}(\mathcal{O}_{32}^{I\,2}+4\mathcal{O}_{33}^{I\,2})\,g_{\mu\nu}$
43	$\Delta^{++}\Delta^{--}Z_{\mu}$	$-\frac{ig}{c_W}(c_W^2-s_W^2)\,(p_1-p_2)_{\mu}$
44	$H^{-}H^{+}Z_{\mu}$	$\frac{ig}{2cW}(s_{\pm}^2(c_W^2-s_W^2)-2s_W^2c_{\pm}^2)\,(p_1-p_2)_{\mu}$
45	$G^{-}G^{+}Z_{\mu}$	$\frac{ig}{2cW}(c_{\pm}^2(c_W^2-s_W^2)-2s_W^2s_{\pm}^2)\,(p_1-p_2)_{\mu}$
46	H_1JZ_{μ}	$-\frac{g}{2cW}(\mathcal{O}_{12}^{R}\mathcal{O}_{12}^{I}-2\mathcal{O}_{13}^{R}\mathcal{O}_{13}^{I})\,(p_1-p_2)_{\mu}$
47	$G^0H_1Z_{\mu}$	$\frac{g}{2cW}(\mathcal{O}_{12}^{R}\mathcal{O}_{22}^{I}-2\mathcal{O}_{13}^{R}\mathcal{O}_{23}^{I})\,(p_1-p_2)_{\mu}$
48	AH_1Z_{μ}	$\frac{g}{2cW}(\mathcal{O}_{12}^{R}\mathcal{O}_{32}^{I}-2\mathcal{O}_{13}^{R}\mathcal{O}_{33}^{I})\,(p_1-p_2)_{\mu}$
49	H_2JZ_{μ}	$-\frac{g}{2cW}(\mathcal{O}_{22}^{R}\mathcal{O}_{12}^{I}-2\mathcal{O}_{23}^{R}\mathcal{O}_{13}^{I})\,(p_1-p_2)_{\mu}$
50	$G^0H_2Z_{\mu}$	$\frac{g}{2cW}(\mathcal{O}_{22}^{R}\mathcal{O}_{22}^{I}-2\mathcal{O}_{23}^{R}\mathcal{O}_{23}^{I})\,(p_1-p_2)_{\mu}$
51	AH_2Z_{μ}	$\frac{g}{2cW}(\mathcal{O}_{22}^{R}\mathcal{O}_{32}^{I}-2\mathcal{O}_{23}^{R}\mathcal{O}_{33}^{I})\,(p_1-p_2)_{\mu}$
52	H_3JZ_{μ}	$-\frac{g}{2cW}(\mathcal{O}_{32}^{R}\mathcal{O}_{12}^{I}-2\mathcal{O}_{33}^{R}\mathcal{O}_{13}^{I})\,(p_1-p_2)_{\mu}$
53	$G^0H_3Z_{\mu}$	$\frac{g}{2cW}(\mathcal{O}_{32}^{R}\mathcal{O}_{22}^{I}-2\mathcal{O}_{33}^{R}\mathcal{O}_{23}^{I})\,(p_1-p_2)_{\mu}$
54	AH_3Z_{μ}	$\frac{g}{2cW}(\mathcal{O}_{32}^{R}\mathcal{O}_{32}^{I}-2\mathcal{O}_{33}^{R}\mathcal{O}_{33}^{I})\,(p_1-p_2)_{\mu}$

Table 3. (Continued.)

	Vertex	Gauge Coupling
55	$G^{\mp}H^{\pm}Z_{\mu}$	$\mp\frac{g}{2c_W}c_{\pm}s_{\pm}\,(p_1-p_2)_{\mu}$
56	$\Delta^{++}\Delta^{--}A_{\mu}A_{\mu}$	$8ie^2\,g_{\mu\nu}$
57	$H^{-}H^{+}A_{\mu}A_{\mu}$	$i2e^2\,g_{\mu\nu}$
58	$G^{-}G^{+}A_{\mu}A_{\mu}$	$i2e^2\,g_{\mu\nu}$
59	$\Delta^{++}\Delta^{--}A_{\mu}$	$-2ie\,(p_1-p_2)_{\mu}$
60	$H^{+}H^{-}A_{\mu}$	$ie\,(p_1-p_2)_{\mu}$
61	$G^{+}G^{-}A_{\mu}$	$ie\,(p_1-p_2)_{\mu}$
62	$\Delta^{++}\Delta^{--}A_{\mu}Z_{\nu}$	$4i\frac{eg}{c_W}(c_W^2-s_W^2)\,g_{\mu\nu}$
63	$H^{+}H^{-}A_{\mu}Z_{\nu}$	$i\frac{eg}{c_W}(s_{\pm}^2(c_W^2-s_W^2)-2c_{\pm}^2s_W^2)\,g_{\mu\nu}$
64	$G^{+}G^{-}A_{\mu}Z_{\nu}$	$i\frac{eg}{c_W}(c_{\pm}^2(c_W^2-s_W^2)-2s_{\pm}^2s_W^2)\,g_{\mu\nu}$

Following our conventions we have that the trilinear coupling $H_2H_1H_1$ turns out to be,

$$\begin{aligned}\frac{g_{H_2H_1H_1}}{2} &= 3\lambda_1(\mathcal{O}^R_{12})^2\mathcal{O}^R_{22}v_2 + 3(\lambda_2+\lambda_4)(\mathcal{O}^R_{13})^2\mathcal{O}^R_{23}v_3 \\ &+ \frac{(\lambda_3+\lambda_5)}{2}[(\mathcal{O}^R_{13})^2\mathcal{O}^R_{22}v_2 + (\mathcal{O}^R_{12})^2\mathcal{O}^R_{23}v_3 + 2\mathcal{O}^R_{12}\mathcal{O}^R_{13}(\mathcal{O}^R_{23}v_2 + \mathcal{O}^R_{22}v_3)] \\ &+ 3\beta_1(\mathcal{O}^R_{11})^2\mathcal{O}^R_{21}v_1 + \frac{\beta_2}{2}[(\mathcal{O}^R_{12})^2\mathcal{O}^R_{21}v_1 + (\mathcal{O}^R_{11})^2\mathcal{O}^R_{22}v_2 + 2\mathcal{O}^R_{11}\mathcal{O}^R_{12}(\mathcal{O}^R_{22}v_1 + \mathcal{O}^R_{21}v_2)] \\ &+ \frac{\beta_3}{2}[(\mathcal{O}^R_{13})^2\mathcal{O}^R_{21}v_1 + (\mathcal{O}^R_{11})^2\mathcal{O}^R_{23}v_3 + 2\mathcal{O}^R_{11}\mathcal{O}^R_{13}(\mathcal{O}^R_{23}v_1 + \mathcal{O}^R_{21}v_3))] \\ &+ \frac{\kappa}{2}[-2\mathcal{O}^R_{11}\mathcal{O}^R_{13}\mathcal{O}^R_{22}v_2 - (\mathcal{O}^R_{12})^2(\mathcal{O}^R_{23}v_1 + \mathcal{O}^R_{21}v_3) - 2\mathcal{O}^R_{12}(\mathcal{O}^R_{13}(\mathcal{O}^R_{22}v_1 + \mathcal{O}^R_{21}v_2) \\ &+ \mathcal{O}^R_{11}(\mathcal{O}^R_{23}v_2 + \mathcal{O}^R_{22}v_3))]. \end{aligned} \tag{34}$$

and hence, for example when $m_{H_1} < 2m_{H_2}$, the decay width $H_2 \to H_1H_1$ is given by

$$\Gamma(H_2 \to H_1H_1) = \frac{g^2_{H_2H_1H_1}}{32\pi m_{H_2}}\left(1 - \frac{4m^2_{H_1}}{m^2_{H_2}}\right)^{1/2}. \tag{35}$$

As we already mentioned, a salient feature of adding an isotriplet to the Standard Modelis that some *visible* decay channels of the Higgs receive further contributions from the charged scalars, namely the one-loop decays $h \to \gamma\gamma$ and $h \to Z\gamma$. That is, the scalars $H^\pm$ and $\Delta^{\pm\pm}$ contribute to the one-loop coupling of the Higgs to two-photons and to Z-photon, leading to deviations from the Standard Modelexpectations for these decay channels. The interactions between CP-even and charged scalars are described by the following vertices,

$$\begin{aligned} H_aH^+H^- &: ig_{H_aH^+H^-} \\ H_a\Delta^{++}\Delta^{--} &: ig_{H_a\Delta^{++}\Delta^{--}} \end{aligned}$$

where

$$\begin{aligned} g_{H_aH^+H^-} &= \frac{1}{2(v_2^2+2v_3^2)}[8\lambda_1\mathcal{O}^R_{a2}v_2v_3^2 + 4(\lambda_2+\lambda_4)\mathcal{O}^R_{a3}v_2^2v_3 + 2\lambda_3(\mathcal{O}^R_{a2}v_2^3 + 2\mathcal{O}^R_{a3}v_3^3) \\ &+ \lambda_5v_2[-2\mathcal{O}^R_{a3}v_2v_3 + \mathcal{O}^R_{a2}(v_2^2 - 2v_3^2)] + 4\beta_2\mathcal{O}^R_{a1}v_1v_3^2 + 2\beta_3\mathcal{O}^R_{a1}v_1v_2^2 \\ &+ 4\kappa v_2v_3(\mathcal{O}^R_{a2}v_1 + \mathcal{O}^R_{a1}v_2)] \\ g_{H_a\Delta^{++}\Delta^{--}} &= 2\lambda_2\mathcal{O}^R_{a3}v_3 + \lambda_3\mathcal{O}^R_{a2}v_2 + \beta_3\mathcal{O}^R_{a1}v_1. \end{aligned}$$

Note that the contributions of $H^\pm$ and $\Delta^{\pm\pm}$ to the decays $h \to \gamma\gamma$ and $h \to Z\gamma$ are functions of the singlet's vev v_1, this is in contrast to what happens in the type-II seesaw model with explicit violation of lepton number. According to equation (26) the dimensionless parameters λ_i and β_i can change the sign of the couplings of $g_{H_aH^+H^-}$ and $g_{H_a\Delta^{++}\Delta^{--}}$, hence the contribution of the charged scalars to $h \to \gamma\gamma$ and $h \to Z\gamma$ may be either constructive or destructive.

For the computation of the decay widths $h \to \gamma\gamma$ and $h \to Z\gamma$ we use the expressions and conventions given in [51]. The decay width $\Gamma(H_a \to \gamma\gamma)$ turns out to be

$$\Gamma(H_a \to \gamma\gamma) = \frac{G_F\alpha^2 m^3_{H_a}}{128\sqrt{2}\pi^3}\,|X_F^{\gamma\gamma} + X_W^{\gamma\gamma} + X_H^{\gamma\gamma}|^2 \tag{36}$$

where G_F is the Fermi constant, α is the fine structure constant and the form factors X_i^j are given by[11],

$$\begin{aligned} X_F^{\gamma\gamma} &= -2C_a\sum_f N_c^f Q_f^2\tau_f[1 + (1-\tau_f)f(\tau_f)], \\ X_W^{\gamma\gamma} &= C_a[2 + \tau_W + 3\tau_W(2-\tau_W)f(\tau_W)] \\ X_H^{\gamma\gamma} &= -\frac{g_{H_aH^+H^-}v}{2\,m^2_{H^\pm}}\tau_{H^\pm}[1 - \tau_{H^\pm}f(\tau_{H^\pm})] - 4\frac{g_{H_a\Delta^{++}\Delta^{--}}v}{2\,m^2_{\Delta^{\pm\pm}}}\tau_{\Delta^{\pm\pm}}[1 - \tau_{\Delta^{\pm\pm}}f(\tau_{\Delta^{\pm\pm}})]. \end{aligned} \tag{37}$$

where $\tau_x = 4m_x^2/m_Z^2$. Here N_c^F and Q_F denote, respectively, the number of colors and electric charge of a given fermion. The one-loop function $f(\tau)$ is defined in appendix B. The parameters C_a correspond to the Standard Model Higgs couplings in equation (28).

[11] We have taken into account that v_3 is very small so that any contribution involving the triplet's vev is neglected. Then for instance the Feynman rule for the vertex $H_aW^+_\mu W^-_\nu$: $i\frac{g^2}{2}(O^R_{a2}v_2 + 2O^R_{a3}v_3)\,g_{\mu\nu}$, is approximated as $\sim i\frac{g^2}{2}(O^R_{a2}v_2)\,g_{\mu\nu}$ (see table 3).

The decay width $\Gamma(H_a \to Z\gamma)$, using the notation in [51], is expressed as follows

$$\Gamma(H_a \to Z\gamma) = \frac{G_F \alpha^2 m_{H_a}^3}{64\sqrt{2}\pi^3}\left(1 - \frac{m_Z^2}{m_{H_a}^2}\right)^3 |X_F^{Z\gamma} + X_W^{Z\gamma} + X_H^{Z\gamma}|^2 \tag{38}$$

where the form factors X_i^j are given by[12],

$$\begin{aligned} X_F^{Z\gamma} &= -4C_a \sum_f N_c^f \frac{g_V^f Q_f m_f^2}{s_W c_W}\left\{\frac{2m_Z^2}{(m_{H_a}^2 - m_Z^2)^2}\Delta B_0^f + \frac{1}{m_{H_a}^2 - m_Z^2}\right. \\ &\quad \left.\times [(4m_f^2 - m_{H_a}^2 + m_Z^2)C_0^f + 2]\right\} \\ X_W^{Z\gamma} &= \frac{C_a}{\tan\theta_W}\left\{\frac{1}{(m_{H_a}^2 - m_Z^2)^2}[m_{H_a}^2(1 - \tan^2\theta_W) - 2m_W^2(-5 + \tan^2\theta_W)]m_Z^2 \Delta B_0^W\right. \\ &\quad + \frac{1}{(m_{H_a}^2 - m_Z^2)}[m_{H_a}^2(1 - \tan^2\theta_W) - 2m_W^2(-5 + \tan^2\theta_W) \\ &\quad \left.+ 2m_W^2[(-5 + \tan^2\theta_W)(m_{H_a}^2 - 2m_W^2) - 2m_Z^2(-3 + \tan^2\theta_W)]C_0^W]\right. \\ X_H^{Z\gamma} &= -2g_{H_a H^+ H^-} v \frac{\tan\theta_W}{(m_{H_a}^2 - m_Z^2)}\left[\frac{m_Z^2}{m_{H_a}^2 - m_Z^2}\Delta B_0^{\pm} + (2m_{H^\pm}^2 C_0^{\pm} + 1)\right] \\ &\quad - 4\frac{g_{H_a \Delta^{++}\Delta^{--}} v}{\tan\theta_W}\frac{(1 - \tan^2\theta_W)}{(m_{H_a}^2 - m_Z^2)}\left[\frac{m_Z^2}{m_{H_a}^2 - m_Z^2}\Delta B_0^{\pm\pm} + (2m_{\Delta^{\pm\pm}}^2 C_0^{\pm\pm} + 1)\right] \end{aligned}$$

where C_0^b and ΔB_0^b are defined in appendix B.

6. Type-II seesaw neutral Higgs searches at the LHC

We stated above that in our study we are assuming $m_{H_1} < m_{H_2} < m_{H_3}$ and $v_1 \gtrsim v_2$. Furthermore, because of the ρ parameter and the astrophysical constraint on the triplet's vev we also have that $v_3 \ll v_1, v_2$. We found that the smallness of v_3 and the perturbativity condition of the potential lead to a very small mixing between the mass eigenstate H_3 and the CP-even components of the fields, σ and Φ, in other words, the angles α_{13} and α_{23} must lie close to 0 or π. As a result, we obtain the following relation,

$$m_{H_3}^2 - m_A^2 \simeq 2\lambda_2 v_3^2 \Longrightarrow m_{H_3} \simeq m_A. \tag{39}$$

This extra mass relation is derived from equation (24), by using equation (25) and the fact that $\alpha_{13,23} \sim 0(\pi)$.

In addition, also as a result of $\alpha_{13,23} \sim 0(\pi)$, we find that the coupling of H_3 to the Standard Modelstates is negligible,

$$\frac{g_{H_3 ff}}{g_{hff}^{\rm SM}} = \frac{g_{H_3 VV}}{g_{hVV}^{\rm SM}} = C_3 \sim 0. \tag{40}$$

In figure 12 of appendix A we give a schematic illustration of the mass profile of the Higgs Bosons in our model. The mass spectrum and composition are summarized in table 2, and provide a useful picture in our following analyses.

6.1. Analysis (i)

In this case we have taken the isotriplet vev $v_3 = 10^{-5}$ GeV, automatically safe from the constraints stemming from astrophysics and the ρ parameter. We have also considered the following mass spectrum,

$$m_{H_1} = [15,\ 115]\ \text{GeV},\quad m_{H_2} = 125\ \text{GeV},\quad m_{H_3} \simeq m_A \simeq m_{H^\pm} \simeq m_{\Delta^{\pm\pm}} = 500\ \text{GeV},$$

and varied the parameters as

$$v_1 \in [100,\ 2500]\ \text{GeV},\quad \alpha_{12} \in [0,\ \pi]\ \text{ and }\ \alpha_{13,23} = \delta_\alpha(\pi - \delta_\alpha) \tag{41}$$

where $0 \leqslant \delta_\alpha < 0.1$. As described in section 4 we must enforce the LEP constraints on the lightest CP-even Higgs H_1 and LHC constraints on the heavier scalars. The near mass degeneracy of H_3, A, $H^\pm$ and $\Delta^{\pm\pm}$ ensures that the oblique parameters are not affected. In analogy to the type-II seesaw model with explicit lepton number violationwe expect that, because of $v_3 < 10^{-4}$ GeV, the doubly-charged scalar predominantly decays into same

[12] Here we have also assumed $v_3 \ll 1$ so as to make the following approximation, $H^+H^-Z_\mu : -ig\sin\theta_W \tan\theta_W (p_+ - p_-)_\mu$.

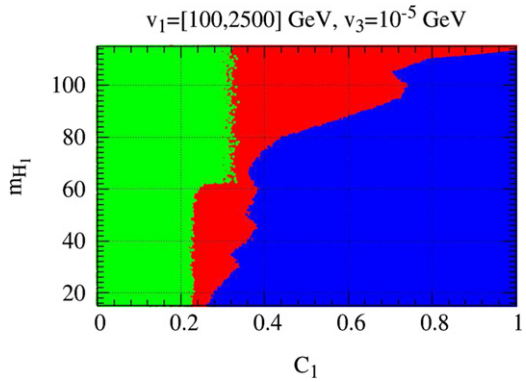

Figure 3. Analysis (i). The mass of the lightest CP-even scalar as a function of the absolute value of its coupling to Standard Model states. The blue region corresponds to the LEP exclusion region and the green (red) one is the LHC allowed (exclusion) region.

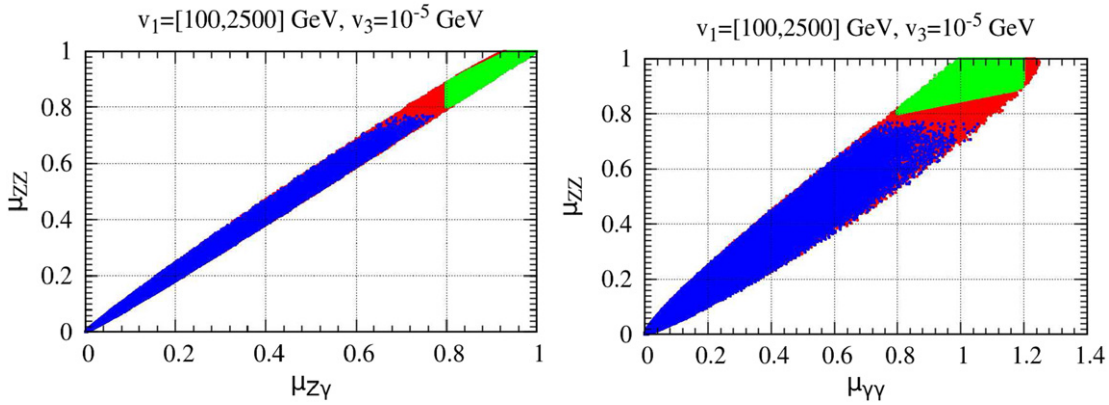

Figure 4. Analysis (i). On the left, we show correlation between μ_{ZZ} and $\mu_{Z\gamma}$. On the right, correlation between μ_{ZZ} and $\mu_{\gamma\gamma}$. The color code as in figure 3.

sign dileptons [41, 44, 45] and that $m_{\Delta^{\pm\pm}} = 500$ GeV is consistent with current experimental data, see section 4.4.

We show in figure 3 the mass of the lightest CP-even scalar as a function of the absolute value of its coupling to the Standard Modelstates, $|C_l|$ in equation (28). The blue region corresponds to the LEP exclusion region and the green(red) one is the LHC allowed(exclusion) region provided by the signal strengths $0.8 < \mu_{XX} < 1.2$.

The presence of light charged scalars can enhance significantly the diphoton channel of the Higgs [39]. Figure 4 shows the correlation between μ_{ZZ} and $\mu_{\gamma\gamma}$ ($\mu_{Z\gamma}$) on the left(right) with $\mu_{\gamma\gamma} \lesssim 1.2$ for charged Higgs Bosons of 500 GeV.

The correlation between the signal strength μ_{ZZ} and the signal strengths $\mu_{\gamma\gamma}$ and $\mu_{Z\gamma}$ is shown in figure 4. Note that the former may exceed one due to the new contributions of the singly and doubly charged Higgs Bosons.

The invisible decays of the Higgs Bosons, characteristic of the model, turn out to be correlated to the visible channels, represented in terms of the signal strengths, as shown in figure 5. Note that the upper bound on the invisible decays of a Higgs Boson with a mass of 125 GeV has been found to be $\mathrm{BR}(H_2 \to \mathrm{Inv}) \lesssim 0.2$. This limit is stronger than those provided by the ATLAS [52] and the CMS [53] collaborations[13].

In figure 6 we depict the correlation between the invisible branching ratios of H_2 with the one of the lightest scalar boson H_1. And, as can be seen, H_1 can decay 100% into the invisible channel (majorons).

Finally, as we have mentioned we obtained that the reduced coupling of H_3 to the Standard Modelstates is $C_3 \sim \mathcal{O}(10^{-7})$ so that it is basically decoupled. As a result its invisible branching is essentially unconstrained, $10^{-5} \lesssim \mathrm{BR}(H_3 \to \mathrm{Inv}) \leqslant 1$. On the other hand we find that the constraint coming from the LHC on the pseudo-scalar A with a mass of 500 GeV is automatically satisfied as well, since from the LHC, $\sigma(gg \to A)\mathrm{BR}(A \to ZH_2)\mathrm{BR}(H_2 \to \tau\tau) \lesssim 10^{-2}$ while for $m_A = 500$ GeV we obtain $\sigma(gg \to A)\mathrm{BR}(A \to ZH_2)\mathrm{BR}(H_2 \to \tau\tau) \lesssim 10^{-15}$.

[13] The ATLAS collaboration has set an upper bound on the BR($H \to$ Inv) at 0.28 while the CMS collaboration reported that the observed (expected) upper limit on the invisible branching ratio is 0.58(0.44), both results at 95% C.L.

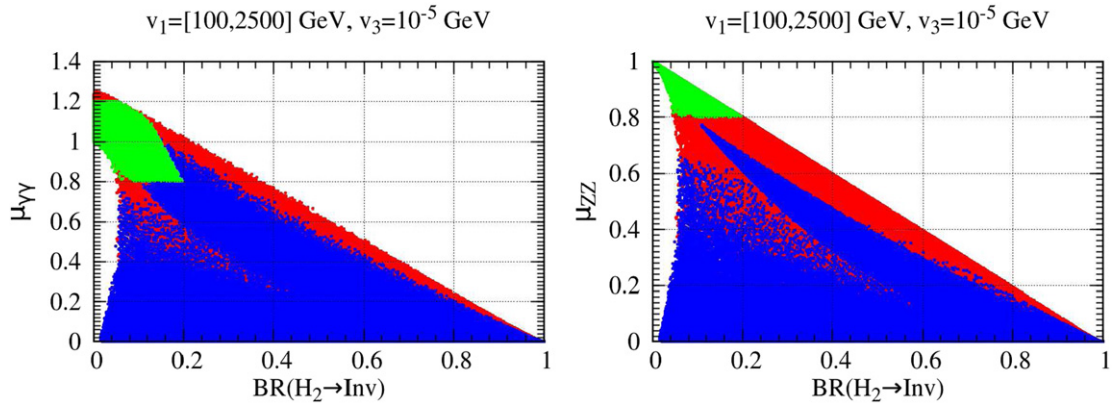

Figure 5. Analysis (i). On the left: the signal strength $\mu_{\gamma\gamma}$ versus BR($H_2 \to$ Inv). On the right: μ_{ZZ} versus BR($H_2 \to$ Inv). The color code as in figure 3.

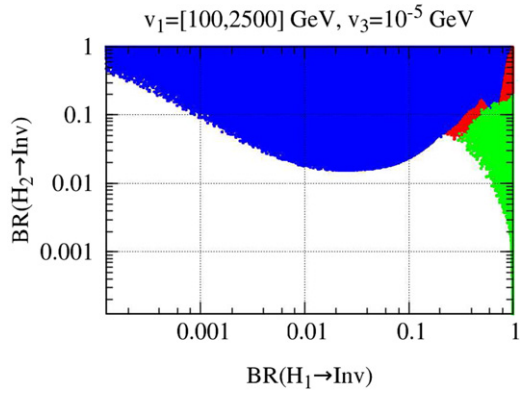

Figure 6. Analysis (i). Correlation between the invible branchings BR($H_2 \to$ Inv) and BR($H_1 \to$ Inv). The color code as in figure 3.

6.2. Analysis (ii)

We now turn to the other case of interest, namely

$$m_{H_1} = 125 \text{ GeV}, \quad m_{H_2} = [150,\ 500] \text{ GeV}, \quad m_{H_3} \simeq m_A \simeq m_{H^\pm} \simeq m_{\Delta^{\pm\pm}} = 600 \text{ GeV},$$

with $v_3 = 10^{-5}$ GeV, as before. Now we scanned over

$$v_1 \in [100,\ 2500] \text{ GeV}, \quad \alpha_{12} \in [0,\ \pi] \quad \text{and} \quad \alpha_{13,23} = \delta_\alpha(\pi - \delta_\alpha) \tag{42}$$

where $0 \leqslant \delta_\alpha < 0.1$. As we already mentioned in this case we only have to take into account the constraints coming from Run 1 of the LHC at 8 TeV, see table 1.

In practice we assume $\mu_{XX} = 1.0^{+0.2}_{-0.2}$. We show in figure 7 the correlation between μ_{ZZ} and $\mu_{\gamma\gamma}$ ($\mu_{Z\gamma}$) on the left(right). As before, the allowed region is in green while the forbidden one is in red. We can see that $\mu_{\gamma\gamma} \lesssim 1.2$ for $m_{H^\pm} \simeq m_{\Delta^{\pm\pm}} = 600$ GeV.

On the left(right) of figure 8 is depicted the correlation between the signal strength μ_{ZZ} ($\mu_{\gamma\gamma}$) and the branching ratio of the channel $H_1 \to JJ$. We can see in figures 8–10 that BR($H_1 \to$ Inv) $\lesssim 0.2$. One can see from figure 9 that BR($H_1 \to$ Inv) $\lesssim 0.1$ for $v_1 \gtrsim 2500$ GeV.

In this case we find that equation (32) (for $\alpha_{13,23} \sim 0(\pi)$ and $v_3 \ll v_1,\ v_2$) at leading order is given by,

$$g_{H_1JJ} \sim \frac{\cos\alpha_{12}}{v_1} m^2_{H_1}, \tag{43}$$

where $m_{H_1} = 125$ GeV. BR($H_1 \to$ Inv) versus the Higgs-majoron coupling g_{H_1JJ} is shown on the right of figure 9. Note also from the left panel in figure 9 that BR($H_1 \to$ Inv) is anti-correlated with v_1, as expected.

In figure 10 we show the correlation between the invisible branching ratio of H_2 (the Higgs with a mass in the range 150 GeV $< m_{H_2} <$ 500 GeV) and the one of H_1.

We have verified that the LHC constraints on the heavy scalars (H_2, H_3 and A) are all satisfied. As an example, the reader can convince her/himself by looking at figure 11 that H_2 easily passes the restriction stemming from

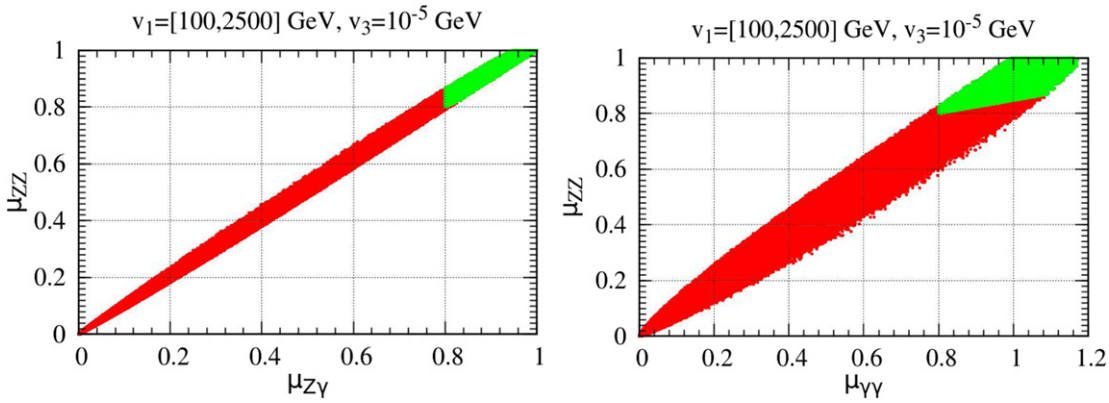

Figure 7. Analysis (ii). On the left, μ_{ZZ} versus $\mu_{Z\gamma}$. On the right, μ_{ZZ} versus $\mu_{\gamma\gamma}$. The allowed region (in green) is the region inside the range $\mu_{XX} = 1.0^{+0.2}_{-0.2}$ while the forbidden one (in red) is the one outside that range.

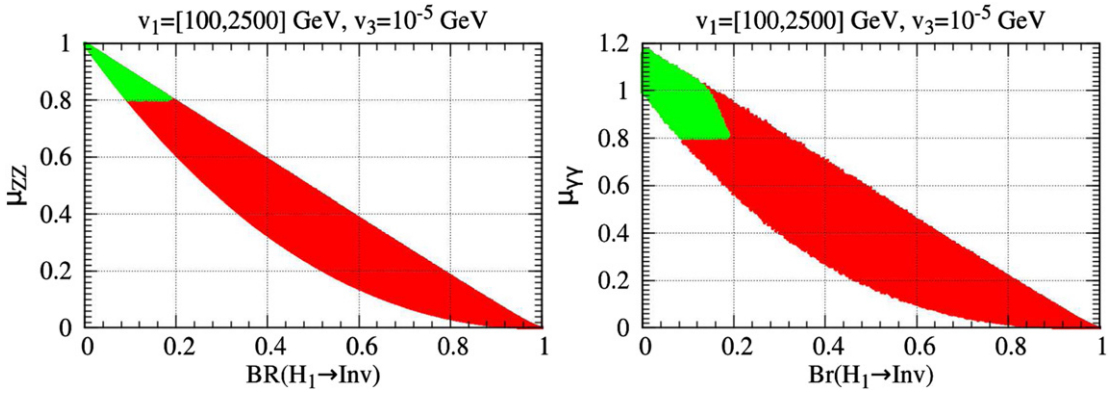

Figure 8. Analysis (ii). On the left: the signal strength μ_{ZZ} versus $\mathrm{Br}(H_1 \to \mathrm{Inv})$. On the right: $\mu_{\gamma\gamma}$ versus $\mathrm{Br}(H_1 \to \mathrm{Inv})$. The color code as in figure 7.

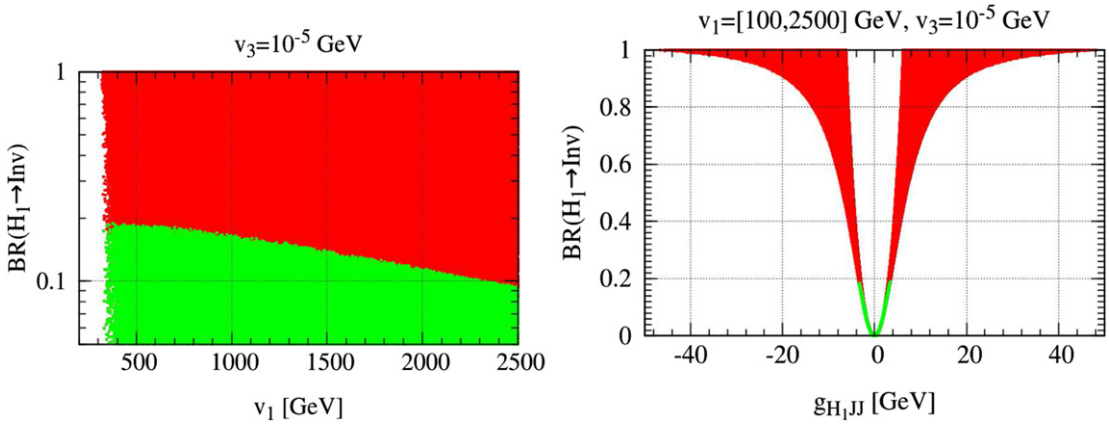

Figure 9. Analysis (ii). $\mathrm{BR}(H_1 \to \mathrm{Inv})$ versus v_1 (on the left) and $\mathrm{BR}(H_1 \to \mathrm{Inv})$ versus the Higgs-majoron coupling g_{H_1JJ} (on the right). The color code as in figure 7.

$\sigma(ggH_2)\mathrm{BR}(H_2 \to \tau\tau)$ (top left) and/or $\sigma(bbH_2)\mathrm{BR}(H_2 \to \tau\tau)$ (top right). The black continuous lines on those plots represent the experimental results from Run 1 of the CMS experiment [30]. We also found that the square of the reduced coupling of H_2 to the Standard Model states is $C_2^2 \lesssim 0.1$ for $m_{H_2} = [150,\ 500]$ GeV. Then, one finds that the experimental upper bounds set by the search for a heavy Higgs in the $H \to WW$ and $H \to ZZ$

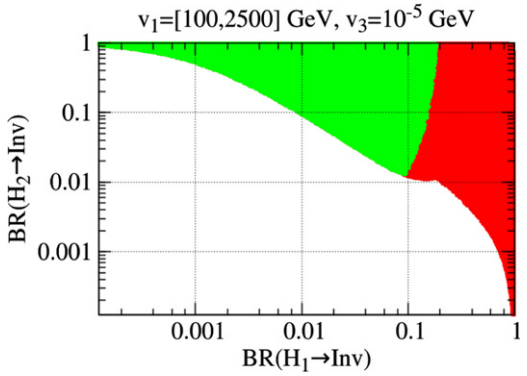

Figure 10. Analysis (ii). Correlation between BR($H_2 \to$ Inv) and BR($H_1 \to$ Inv). The color code as in figure 7.

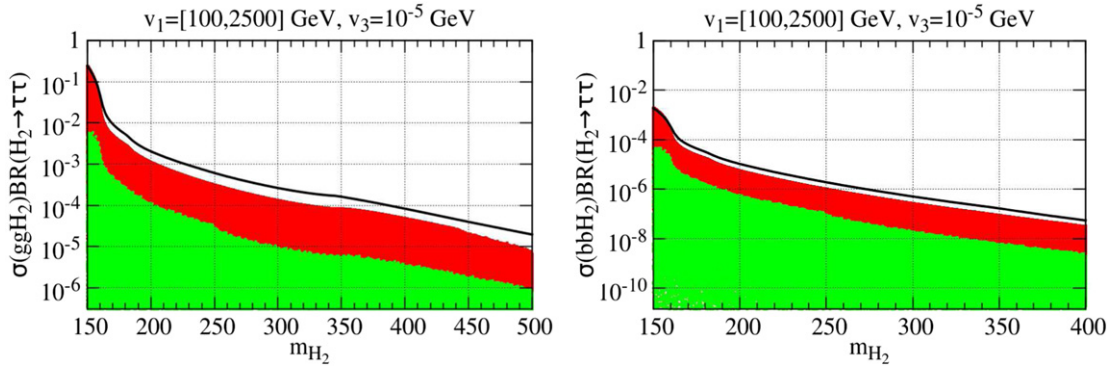

Figure 11. Analysis (ii). On the top right (left) $\sigma\,(ggH_2)\,\mathrm{BR}(H_2 \to \tau\tau)$ ($\sigma\,(bbH_2)\,\mathrm{BR}(H_2 \to \tau\tau)$) versus the mass of H_2.

decay channels in [3, 29] are automatically fulfilled. However, improved sensitivities expected from Run 2 may provide a meaningful probe of the theoretically consistent region, depicted in green.

Also in this case, H_3 is decoupled, so the restrictions on H_3 and the massive pseudoscalar A are automatically fulfilled.

7. Conclusions

In this paper we have presented the main features of the electroweak symmetry breaking sector of the simplest type-II seesaw model with spontaneous violation of lepton number. The Higgs sector has two characteristic features: (a) the existence of a (nearly) massless Nambu–Goldstone boson and (b) all neutral CP-even and CP-odd, as well as singly and doubly-charged scalar bosons coming mainly from the triplet are very close in mass, as illustrated in figure 12 of appendix A. However, one extra CP-even state, namely H_2 coming from a doublet-singlet mixture can be light. After reviewing the 'theoretical' and experimental restrictions which apply on the Higgs sector, we have studied the sensitivities of the searches for Higgs Bosons at the ongoing ATLAS/CMS experiments, including not only the new contributions to Standard Modeldecay channels, but also the novel Higgs decays to majorons. For these we have considered two cases, when the 125 GeV state found at CERN is either (i) the second-to-lightest or (ii) the lightest CP-even scalar boson. For case (i), we have enforced the constraints coming from LEP-II data on the lightest CP-even scalar coupling to the Standard Modelstates and those coming from the LHC Run-1 on the heavier scalars. In case (ii), only the constraints coming from the LHC must be taken into account. Such 'invisible' Higgs Boson decays give rise to missing momentum events. We have found that the experimental results from Run 1 on the search for a heavy Higgs in the $H \to WW$ and $H \to ZZ$ decay channels are automatically fulfilled. However, improved sensitivities expected from Run 2 may provide a meaningful probe of this scenario. In short we have discussed how the neutrino mass generation scenario not only suggests the need to reconsider the physics of electroweak symmetry breaking from a new perspective, but also provides a new theoretically consistent and experimentally viable paradigm.

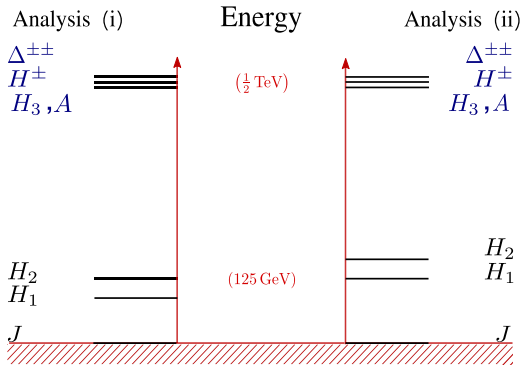

Figure 12. Type-II seesaw Higgs Boson mass spectrum.

Acknowledgments

Work supported by the Spanish grants FPA2014-58183-P, Multidark CSD2009-00064 and SEV-2014-0398 (MINECO), and PROMETEOII/2014/084 (Generalitat Valenciana). CB thanks Departamento de Física and CFTP, Instituto Superior Técnico, Universidade de Lisboa, for its hospitality while part of this work was carried out. JCR is also support in part by the Portuguese Fundação para a Ciência e Tecnologia (FCT) under contracts UID/FIS/00777/2013 and CERN/FIS-NUC/0010/2015, which are partially funded through POCTI (FEDER), COMPETE, QREN and the EU.

Appendix A. Higgs Boson mass spectrum

Appendix B. Loop functions

The one-loop function $f(\tau)$ used in equation (37) is given by,

$$f(\tau) = \begin{cases} \arcsin^2(1/\sqrt{\tau}) & \text{if } \tau \geqslant 1 \\ -\frac{1}{4}\left[\log\left(\frac{1+\sqrt{1-\tau}}{1-\sqrt{1-\tau}}\right) - i\pi\right]^2 & \text{if } \tau < 1 \end{cases} \tag{B1}$$

The functions C_0^b and ΔB_0^b are given in terms of the Passarino–Veltman functions [54],

$$\begin{aligned} C_0^b &= C_0(m_Z^2,\, 0,\, m_{H_a}^2,\, m_b^2,\, m_b^2,\, m_b^2) = -\frac{1}{m_b^2} I_2(\tau_b,\, \lambda_b), \\ \Delta B_0^b &= B_0(m_{H_a}^2,\, m_b^2,\, m_b^2) - B_0(m_Z^2,\, m_b^2,\, m_b^2) \\ &= -\frac{m_{H_a}^2 - m_Z^2}{m_Z^2} - \frac{(m_{H_a}^2 - m_Z^2)^2}{2m_a^2 m_Z^2} I_1(\tau_b,\, \lambda_b) + 2\frac{m_{H_a}^2 - m_Z^2}{m_Z^2} I_2(\tau_b,\, \lambda_b) \end{aligned} \tag{B2}$$

where $\lambda_b = 4m_b^2/m_{H_a}^2$,

$$\begin{aligned} I_1(\tau,\, \lambda) &= \frac{\tau\lambda}{2(\tau-\lambda)} + \frac{\tau^2\lambda^2}{2(\tau-\lambda)^2}[f(\tau) - f(\lambda)] + \frac{\tau^2\lambda}{(\tau-\lambda)^2}[g(\tau) - g(\lambda)], \\ I_2(\tau,\, \lambda) &= -\frac{\tau\lambda}{2(\tau-\lambda)}[f(\tau) - f(\lambda)], \end{aligned} \tag{B3}$$

and

$$g(\tau) = \begin{cases} \sqrt{\tau-1}\arcsin\sqrt{\tau} & \text{for } \tau \geqslant 1 \\ \frac{1}{2}\sqrt{1-\tau}\left(\log\frac{1+\sqrt{1-\tau}}{1-\sqrt{1-\tau}} - i\pi\right) & \text{if } \tau < 1 \end{cases} \tag{B4}$$

Appendix C. Higgs Boson couplings

References

[1] Aad G *et al* (ATLAS Collaboration) 2012 Observation of a new particle in the search for the Standard Model Higgs Boson with the ATLAS detector at the LHC *Phys. Lett.* B **716** 1–29
[2] Aad G *et al* 2016 Measurements of the Higgs boson production and decay rates and coupling strengths using pp collision data at $\sqrt{s} = 7$ and 8 TeV in the ATLAS experiment *Eur. Phys. J.* C **76** 6
[3] Khachatryan V *et al* 2015 (CMS), Precise determination of the mass of the Higgs Boson and tests of compatibility of its couplings with the standard model predictions using proton collisions at 7 and 8 TeV *Eur. Phys. J.* C **75** 212
[4] Aad G *et al* 2015 Measurements of Higgs boson production and couplings in the four-lepton channel in pp collisions at center-of-mass energies of 7 and 8 TeV with the ATLAS detector *Phys. Rev.* D **91** 012006
[5] Baak M *et al* 2012 The electroweak fit of the Standard Model after the discovery of a new boson at the LHC *Eur. Phys. J.* C **72** 2205
[6] Baak M *et al* (Gfitter Group) 2014 The global electroweak fit at NNLO and prospects for the LHC and ILC *Eur. Phys. J.* C **74** 3046
[7] Peskin M E and Takeuchi T 1990 New constraint on a strongly interacting higgs sector *Phys. Rev. Lett.* **65** 964–7
[8] Altarelli G and Barbieri R 1991 Vacuum polarization effects of new physics on electroweak processes *Phys. Lett.* B **253** 161–7
[9] Peskin M E and Takeuchi T 1992 Estimation of oblique electroweak corrections *Phys. Rev.* D **46** 381–409
[10] Djouadi A 2008 The Anatomy of electro-weak symmetry breaking: I. The Higgs Boson in the standard model *Phys. Rept* **457** 1–216
[11] Bonilla C, Fonseca R M and Valle J W F 2015 Vacuum stability with spontaneous violation of lepton number (arXiv:1506.04031)
[12] Bonilla C, Fonseca R M and Valle J W F 2015 Consistency of the triplet seesaw model revisited *Phys. Rev.* D **92** 075028
[13] Bonilla C, Valle J W F and Romo J C 2015 Neutrino mass and invisible Higgs decays at the LHC *Phys. Rev.* D **91** 113015
[14] Schechter J and Valle J 1982 Neutrino Decay and Spontaneous Violation of Lepton Number *Phys. Rev.* D **25** 774
[15] Joshipura A S and Valle J 1993 Invisible Higgs decays and neutrino physics *Nucl. Phys.* B **397** 105–22
[16] Diaz M A, Garcia-Jareno M, Restrepo D A and Valle J 1998 Seesaw Majoron model of neutrino mass and novel signals in Higgs Boson production at LEP *Nucl. Phys.* B **527** 44–60
[17] Chikashige Y, Mohapatra R N and Peccei R 1981 Are there real goldstone bosons associated with broken Lepton number? *Phys. Lett.* B **98** 265
[18] Gelmini G and Roncadelli M 1981 Left-handed neutrino mass scale and spontaneously broken Lepton number *Phys. Lett.* B **B99** 411
[19] Shrock R E and Suzuki M 1982 Invisible decays of Higgs Bosons *Phys. Lett.* B **110** 250
[20] Boucenna S M, Morisi S and Valle J W 2014 The low-scale approach to neutrino masses *Adv. High Energy Phys.* **2014** 831598
[21] Schechter J and Valle J 1980 Neutrino masses in SU(2) x U(1) theories *Phys. Rev.* D **22** 2227
[22] Kannike K 2012 Vacuum stability conditions from copositivity criteria *Eur. Phys. J.* C **72** 2093
[23] Olive K A *et al* (Particle Data Group) 2014 Review of particle physics *Chin. Phys.* C **38** 090001
[24] Choi K and Santamaria A 1990 Majorons and supernova cooling *Phys. Rev.* D **42** 293–306
[25] Khachatryan V *et al* (CMS Collaboration) 2014 Observation of the diphoton decay of the Higgs Boson and measurement of its properties *Eur. Phys. J* C **74** 3076
[26] Aad G *et al* (ATLAS, CMS) 2015 Combined measurement of the Higgs Boson mass in ıt pp Collisions at $\sqrt{s} = 7$ and 8 TeV with the ATLAS and CMS experiments *Phys. Rev. Lett.* **114** 191803
[27] Abdallah J *et al* (DELPHI Collaboration) 2004 Searches for neutral Higgs Bosons in extended models *Eur. Phys. J.* C **38** 1–28
[28] Measurements of the Higgs Boson production and decay rates and constraints on its couplings from a combined ATLAS and CMS analysis of the LHC pp collision data at $\sqrt{s} = 7$ and 8 TeV, Technical Report ATLAS-CONF-2015-044, CERN, Geneva (2015) (http://cds.cern.ch/record/2052552)
[29] Khachatryan V *et al* 2015 Search for a Higgs Boson in the mass range from 145 to 1000 GeV decaying to a pair of W or Z bosons (arXiv:1504.00936) [hep-ex]
[30] Khachatryan V *et al* (CMS) 2014 Search for neutral MSSM Higgs Bosons decaying to a pair of tau leptons in pp collisions *J High Energy Phys.* JHEP10(2014)160
[31] Aad G *et al* (ATLAS) 2014, Search for scalar diphoton resonances in the mass range 65−600 GeV with the ATLAS detector in pp collision data at $\sqrt{s} = 8$ TeV *Phys. Rev. Lett.* **113** 171801
[32] Khachatryan V *et al* 2015 (CMS), Search for diphoton resonances in the mass range from 150 to 850 GeV in pp collisions at $\sqrt{s} = 8$ TeV *Phys. Lett.* B **750** 494–519
[33] Aad G *et al* (ATLAS) 2015 Search for a CP-odd Higgs Boson decaying to Zh in pp collisions at $\sqrt{s} = 8$ TeV with the ATLAS detector *Phys. Lett.* B **744** 163–83
[34] Garayoa J and Schwetz T 2008 Neutrino mass hierarchy and Majorana CP phases within the Higgs triplet model at the LHC *J High Energy Phys.* JHEP03(2008)009
[35] Perez P Fileviez *et al* 2008 Testing a neutrino mass generation mechanism at the LHC *Phys. Rev.* D **78** 071301
[36] Fileviez Perez P *et al* 2008 Neutrino masses and the CERN LHC: testing type II seesaw *Phys.Rev.* D **78** 015018
[37] del Aguila F and Aguilar-Saavedra J A 2009 Distinguishing seesaw models at LHC with multi-lepton signals *Nucl. Phys.* B **813** 22–90
[38] Aoki M, Kanemura S and Yagyu K 2012 Testing the Higgs triplet model with the mass difference at the LHC *Phys. Rev.* D **85** 055007
[39] Akeroyd A G and Moretti S 2012 Enhancement of H to gamma gamma from doubly charged scalars in the Higgs Triplet Model *Phys. Rev.* D **86** 035015
[40] Dev P S B, Ghosh D K, Okada N and Saha I 2013 125 GeV Higgs Boson and the Type-II Seesaw Model *J. High Energy Phys.* **03** JHEP03(2013)150
Dev P S B, Ghosh D K, Okada N and Saha I 2013 *J. High Energy Phys.* JHEP05(2013)049
[41] del Águila F and Chala M 2014 LHC bounds on Lepton number violation mediated by doubly and singly-charged scalars *J. High Energy Phys.* JHEP03(2014)027
[42] Chen C-H and Nomura T 2015 Search for $\delta^{\pm\pm}$ with new decay patterns at the LHC *Phys. Rev.* D **91** 035023
[43] Kanemura S, Kikuchi M, Yagyu K and Yokoya H 2014 Bounds on the mass of doubly-charged Higgs Bosons in the same-sign diboson decay scenario *Phys. Rev.* D **90** 115018
[44] Han Z-L, Ding R and Liao Y 2015 LHC Phenomenology of type II seesaw: nondegenerate case *Phys. Rev.* D **91** 093006

[45] Sugiyama H, Tsumura K and Yokoya H 2014 Discrimination of models including doubly charged scalar bosons by using tau lepton decay distributions *Phys. Lett.* B **717** 229–34
[46] Chatrchyan S *et al* 2012 (CMS), A search for a doubly-charged Higgs Boson in pp collisions at $\sqrt{s} = 7$ TeV *Eur. Phys. J.* C **72** 2189
[47] Aad G *et al* 2012 Search for doubly-charged Higgs Bosons in like-sign dilepton final states at $\sqrt{s} = 7$ TeV with the ATLAS detector *Eur. Phys. J.* C **72** 2244 (ATLAS)
[48] Kanemura S, Yagyu K and Yokoya H 2013 First constraint on the mass of doubly-charged Higgs Bosons in the same-sign diboson decay scenario at the LHC *Phys. Lett.* B **726** 316–9
[49] Kanemura S, Kikuchi M, Yokoya H and Yagyu K 2015 LHC Run-I constraint on the mass of doubly charged Higgs Bosons in the same-sign diboson decay scenario *PTEP* **2015** 051B02
[50] Khachatryan V *et al* (CMS) 2015 Study of vector boson scattering and search for new physics in events with two same-sign leptons and two jets *Phys. Rev. Lett.* **114** 051801
[51] Fontes D, Romão J C and Silva J P 2014 $h \to Z\gamma$ in the complex two Higgs doublet model *J. High Energy Phys.* JHEP02(2014)043
[52] Aad G *et al* 2015 Search for invisible decays of a Higgs Boson using vector-boson fusion in pp collisions at TeV with the ATLAS detector (arXiv:1508.07869)
[53] Chatrchyan S *et al* (CMS) 2014 Search for invisible decays of Higgs Bosons in the vector boson fusion and associated ZH production modes *Eur. Phys. J.* C **74** 2980
[54] Passarino G and Veltman M J G 1979 One loop corrections for e^+e^- annihilation into $\mu^+\mu^-$ in the Weinberg model *Nucl. Phys.* B **160** 151–207